



Published in final edited form as:

Pain. 2014 January ; 155(1): 137–149. doi:10.1016/j.pain.2013.09.020.

Irritable Bowel Syndrome in female patients is associated with alterations in structural brain networks

Jennifer Labus^{1,4}, Ivo D. Dinov², Zhiguo Jiang¹, Cody Ashe-McNalley¹, Alen Zamanyan², Yonggang Shi², Jui-Yang Hong¹, Arpana Gupta¹, Kirsten Tillisch¹, Bahar Ebrat¹, Sam Hobel², Boris A. Gutman², Shantanu Joshi², Paul M. Thompson², Arthur W. Toga², and Emeran A. Mayer^{1,3,4}

¹Oppenheimer Family Center for Neurobiology of Stress, Pain and Interoception Network (PAIN), David Geffen School of Medicine at UCLA, Los Angeles, CA 90095

²Laboratory of Neuro Imaging (LONI), Department of Neurology, University of California, Los Angeles, Los Angeles, CA 90095

³Ahmanson-Lovelace Brain Mapping Center, UCLA

⁴Brain Research Institute, UCLA

Abstract

Alterations in gray matter (GM) density/ volume and cortical thickness (CT) have been demonstrated in small and heterogeneous samples of subjects with different chronic pain syndromes, including irritable bowel syndrome (IBS). Aggregating across 7 structural neuroimaging studies conducted at UCLA between August 2006 and April 2011, we examined group differences in regional GM volume in 201 predominantly premenopausal female subjects (82 IBS, mean age: 32 ± 10 SD, 119 Healthy Controls [HCs], 30 ± 10 SD). Applying graph theoretical methods and controlling for total brain volume, global and regional properties of large-scale structural brain networks were compared between IBS and HC groups. Relative to HCs, the IBS group had lower volumes in bilateral superior frontal gyrus, bilateral insula, bilateral amygdala, bilateral hippocampus, bilateral middle orbital frontal gyrus, left cingulate, left gyrus rectus, brainstem, and left putamen. Higher volume was found for the left postcentral gyrus. Group differences were no longer significant for most regions when controlling for Early Trauma

© 2013 International Association for the Study of Pain. Published by Elsevier B.V. All rights reserved.

Correspondence: Jennifer Labus, Ph.D., Oppenheimer Family Center for Neurobiology of Stress, UCLA CHS 47-230; MC 737818, 10833 Le Conte Ave, Los Angeles, CA 90095-7378.

Publisher's Disclaimer: This is a PDF file of an unedited manuscript that has been accepted for publication. As a service to our customers we are providing this early version of the manuscript. The manuscript will undergo copyediting, typesetting, and review of the resulting proof before it is published in its final citable form. Please note that during the production process errors may be discovered which could affect the content, and all legal disclaimers that apply to the journal pertain.

Authors' contributions

All authors made substantive intellectual contributions to this research and development effort including the article conception, study design, data processing, drafting and revising the final manuscript.

The authors have no conflicts of interest to disclose.

As of September 2013, the Laboratory of Neuro Imaging (LONI) will be relocated to the University of Southern California (USC). Thus, some of the URL links, web-page references, and internet resources cited throughout this manuscript may be relocated to appropriate subdomains under <http://www.loni.usc.edu>. If you find broken links or defunct URLs please contact help@loni.usc.edu.

Inventory global score with the exception of the right amygdala and the left post central gyrus. No group differences were found for measures of global and local network organization. Compared to HCs, the right cingulate gyrus and right thalamus were identified as significantly more critical for information flow. Regions involved in endogenous pain modulation and central sensory amplification were identified as network hubs in IBS. Overall, evidence for central alterations in IBS was found in the form of regional GM volume differences and altered global and regional properties of brain volumetric networks.

Keywords

chronic pain; irritable bowel syndrome; gray matter volume; brain network analysis; graph theory

1.1.0. Introduction

Structural alterations of the brain in the form of higher or lower gray matter (GM) density and volume and cortical thickness (CT) have been reported in a wide range of chronic somatic and visceral pain conditions, including chronic inflammatory conditions (osteoarthritis [6; 107], chronic pancreatitis [49; 128], Crohn's disease [2]), persistent often comorbid pain syndromes (temporomandibular disorder [51; 54; 95; 115; 144], vulvodinia [115], chronic pelvic pain [5; 97], irritable bowel syndrome [12; 35; 116], fibromyalgia [20; 75; 143]), migraine [71; 106; 111; 141], chronic tension-type headache [113], cyclical menstrual pain [138]) and other pain conditions (chronic lower back pain [4; 99; 112; 139], complex regional pain syndrome [50; 53; 54; 99].) The variability in reported findings may be in part related to the fact that the majority of these studies were relatively small, and poorly controlled for medication intake, the presence of comorbid conditions, or sex. The most commonly reported regions with lower GM were subregions of cingulate and insular cortices, temporal lobe, prefrontal cortex and thalamus/basal ganglia [34; 88], while disease related regional GM volume increases have been reported in a few studies [94; 115; 116], involving basal ganglia, hippocampus, anterior cingulate (ACC) subregions, posterior insula, and somatosensory cortex (S1). Previously published reports suggest different patterns of grey matter changes for different types of chronic pain, such as neuropathic and nociceptive pain [53; 54].

Recent research examining GM morphometry (volume, surface area, cortical thickness), anatomical connectivity (white matter tractography) and brain function (resting state, task-based) indicate that disease related symptoms may be associated with altered integration of brain regions that comprise large-scale networks [8; 9; 17; 19; 26; 57–59; 108; 110]. In studies examining GM morphometry, anatomical connectivity is inferred from correlated regional GM measures (e.g., volumes). Correlation of anatomic features of brain regions across individuals may partly reflect functional interactions between these areas [19; 121], mutually trophic effects on growth mediated by axonal connections [45–47], tissue type similarities [19; 27], genetics [24; 45; 114; 130], and/or environment-related plasticity [1; 45; 92; 114].

We aggregated data across 7 structural neuroimaging studies conducted at UCLA between August 2006 and April 2011, and examined group differences in regional GM volume in a

large sample of 201 female subjects (82 IBS, 119 HCs). We applied network analysis to obtain new insights about large-scale regional connectivity and to compare morphological brain architectures and network properties between groups of IBS and HC subjects. To assist in our large-scale analyses we employed the Laboratory of Neuro Imaging (LONI) pipeline [39; 41; 136], a graphical workflow environment which allows users to describe executable tools in a graphical user interface and create processing modules as nodes in a graph representing the complete computational protocol [40; 42]. We provide evidence for both regional alterations in GM volume, as well as differences in regional properties of large scale structural brain networks in IBS compared to HCs.

2.1.0. Methods

2.1.1. Subjects—Female IBS and HC subjects were recruited from multiple clinical sites at UCLA, which are part of the clinical research network of the Center for Neurobiology of Stress, and from community advertisements. A diagnosis of IBS was made using the ROME II or III symptom criteria [86; 131] based on assessments by gastroenterologists experienced in the diagnosis of functional bowel disease and the exclusion of organic disease. A gastroenterologist or GI nurse practitioner obtained a history and conducted a physical examination. IBS patients with all types of predominant bowel habits were included. Using clinical histories or questionnaire data, subjects with a history of any chronic functional symptom or syndrome, or symptoms suggestive of disordered mood or affect were excluded. Potential subjects were also excluded if they a) had a serious medical condition or were taking medications, as this may interfere with interpretation of the brain imaging or physiological measures; b) had an ongoing major psychiatric diagnosis or were being treated with psychotropic medication being used over the past 6 months (subjects were not excluded for lifetime incidence of psychiatric disorders, or for intake of low dose tricyclic antidepressants for non-psychiatric indication); c) engaged in excessive physical exercise (i.e. marathon runners).

2.1.2. Structural MRI—Brain images from 201 females (82 IBS, 119 HCs) were obtained and combined from 7 structural imaging studies conducted at UCLA using four separate protocols. Included in this subject pool, were 55 IBS and 48 HCs included in a prior analysis of GM density using voxel-based morphometry [116]. Brain images were acquired on 1.5 or 3T MRI scanners (Siemens Allegra). First, a sagittal scout was used to position the head. Then each subject underwent one of 4 structural acquisition sequences using a high-resolution 3-dimensional T1-weighted, sagittal, magnetization prepared rapid gradient echo (MP-RAGE) protocol. See Tables 1 and 2 for a description of the structural acquisition protocols.

2.1.3. Phenotype data—We collected phenotyping data on early adverse life events (EALs) (early trauma inventory; ETI) [15], trait anxiety scores (State Trait Anxiety Inventory; STAI) [122], depression and anxiety (Hospital Anxiety and Depression Scale; HAD) [145], catastrophizing (Coping Strategies Questionnaire; CSQ) [105], and health status (Patient Health Questionnaire; PHQ, using 12 items without GI related questions) [73]. IBS symptom severity, abdominal pain and duration in the past week were measured

on a 21-point numeric rating scale (Bowel Symptoms Questionnaire; BSQ) [98]. Usual symptom severity was assessed on an ordinal scale (1=None; 2=Mild; 3=Moderate; 4=Severe; 5=Very Severe). Menopause status was assessed by self-report.

2.2.0. Data Analyses

2.2.1. Volumetric Analysis—The LONI (UCLA Laboratory of Neuroimaging) pipeline was used for image preprocessing and volumetric analysis. Figure 1 shows the pipeline workflow implementing the volumetric data analysis. The volumetric workflow pipeline consists of 4 main components— data preprocessing (intensity inhomogeneity correction [118] and skull-stripping [83; 84], cortical surface modeling [48], and tissue classification [134; 135]. The complete pipeline workflows are available as XML objects which can be downloaded, viewed and tested via the Pipeline environment (pipeline.loni.ucla.edu), see supplementary Files 1 and 2.

2.2.2. Brain Parcellation—Global and regional volumetric analyses rely on dividing the brain into both its different tissues and 56 predefined brain structures based on the LONI probabilistic brain atlas (LBPA 40) [118] using SVPAsseg [134; 135]. In order to analyze additional subcortical brain regions not delineated by the above method, we applied FSL FMRIB's Integrated Registration and Segmentation Tool (FIRST v1.2) [66; 120], and the Harvard-Oxford atlas (amygdala, thalamus, nucleus accumbens) [37]. Table 3 contains the list of regions and an interactive LBP40 atlas parcellation depicting these regions can be examined at <http://scalablebrainatlas.incf.org/main>. For each tissue or brain structure the individual volume was measured by the voxel dimensions (1×1×1 mm) multiplied by the number of voxels within the segmented structure, revealing total brain volume (TBV), whole-brain grey matter (GM) volume or other regional volume. For each subject, regions of interest (ROIs) were visually inspected (using 3D viewer) after the brain parcellation. Then the across-subjects distributions volumetric measures defined on the 56 ROIs were quantitatively generated and inspected. Linear contrasts analyses on the estimates from a general linear model (GLM) were used to compare potential protocol differences in tissue classification controlling for group differences. The raw probability values of rejecting the null hypothesis due to chance alone (p-values) were adjusted for multiple comparisons, yielding a q-value, using a publicly available tool (<http://users.ox.ac.uk/~npike/fdr/>) to implement a graphically sharpened method for controlling false discovery rate at 5% (number of comparison=6) [103].

2.2.3. Regions of Interest (ROI) for volumetric group comparisons—To examine group differences and brain-symptom correlations, ROIs were selected based on functional neuroimaging studies in IBS, which have examined key regions of homeostatic afferent (interoceptive), emotional arousal and cognitive modulatory brain circuits [78; 79; 132; 133]. Briefly, the homeostatic afferent network is comprised of regions central for processing of viscerosensory information including thalamus, insula (posterior, mid, anterior), dorsal anterior cingulate [ACC] subregions [30; 31; 76; 79; 91]. The emotional arousal network includes amygdala, anterior insula, ACC subregions (including sub and pregenual), and dorsal pons (including the locus coeruleus complex) [62; 77; 102; 127; 132; 140]. The cognitive modulatory network reflects the modulating influence of cortical

regions (i.e. prefrontal, parietal) on the homeostatic afferent and emotional arousal networks [78; 90; 100]. From the LPBA 40 atlas [117], we examined superior, inferior and middle frontal gyrus, lateral and middle orbitofrontal gyrus (mOFG), cingulate, insula, brainstem, parahippocampal gyrus, gyrus rectus, hippocampus, putamen, and post central gyrus; and from the Harvard-Oxford atlas we examined amygdala, and thalamus.

Group differences in ROI volumes were determined using the general linear model (GLM) and linear contrast analysis controlling for TBV in SPSS v19. To determine if variations in group differences were explained by covariates trait anxiety (STAI) and early life trauma (ETI), we recalculated the original GLMs after adding each single covariate. Inspection of STAI and ETI indicated positive skewness in these measures. As such in order to improve the normality of the distribution, we transformed these scores using the square root transformation. We implemented the aforementioned graphically sharpened method for controlling false discovery rate at 5% (number of comparison=29) [103]. We quantify group differences by calculating Cohen's *d* reflecting the difference between HCs and IBS scale of standard deviation units. As a rule of thumb, an effect size of $g=.80$ is considered large (explaining 14% of the variance), $.50$ medium (6% variance explained), and $.20$ small (1% variance explained).

In IBS, exploratory partial correlation analyses were conducted, controlling for total GM volume and age, in order to examine the relationship between regional GM volume and the continuous symptom measures data assessed by the BSQ, overall symptom severity and abdominal pain in the past week and chronicity of IBS symptoms.

2.2.4 Complex Network Analysis—For a detailed description of brain network measures see [108]. To investigate alterations in the architecture of structural networks in IBS compared to HCs we applied graph theoretical methods using the Graph Analysis Toolbox [60], which integrates the Brain Connectivity toolbox [108] for computing network measures. The analytical pipeline is depicted in Figure 2. Controlling for TBV with the linear regression, inter-regional volume based correlation matrices were computed for the 62 regional volumes for each group based on the parcellations using the LPBA 40 and Harvard-Oxford atlases. Volumetric-based brain networks were then constructed by binarizing the correlation matrices based on the minimum network density threshold in each group. The minimum density threshold is the correlation value at which all the regions or nodes of the network are fully connected to the brain networks in each group (i.e., none of the networks are fragmented). Choosing to threshold at the minimum density ensures results are not influenced by group differences in average degree and connection density. *Density* is the ratio of the number of connections present to the number of possible connections and is a measure of *wiring cost*. The connectivity or wiring of regions is thought to be based on the principle of wiring minimization and cost efficiency which permits the most economical use of space and energy (metabolic costs) in the brain [18]. *Minimum density* reflects the minimum *wiring cost* possible before network fragmentation (See INSET Figure 2). Consistent with previous studies [60; 61; 85], we chose the *minimum density* value to threshold the networks. However, because choice of threshold can affect measures of network topology [142], we applied a sensitivity analysis to examine global network properties at a range of *wiring costs* or *densities*, $.05$ to $.45$. The binarized matrices entered

as data in the analysis are called *adjacency* or connection matrices and an entry of 1 reflects presence of a connection ($r \geq$ minimum density) and 0 reflects absence of a connection ($r <$ minimum density).

After generating the structural brain networks, network measures that characterize global and local brain efficiency were computed. Specifically, we examined the *small-world attributes* of the structural networks by examining the *clustering coefficient*, *characteristic path length*, and the *small-worldness* index. The *clustering coefficient* of a region quantifies the probability that the regions a particular brain region is connected to are also connected to each other. Averaging the *cluster coefficient* across all regions produces the *network's clustering coefficient*, which is considered an indicator of network segregation.

Characteristic path length refers to the average number of distinct *paths* (also called edges) for a signal to travel between two regions. A short *path length* indicates that a brain region can be reached from another region through a *path* composed of only a few connections. High clustering (i.e., complexity) and short *path lengths* (i.e., wiring) are properties of small-world attributes [123; 124]. We assessed *modularity* of the network, where higher *modularity* reflects several densely connected nodes and fewer connections between nodes in a different module [93]. In addition, *global efficiency* was quantified by using the inverse of the distance matrix, which represents the shortest possible *path* from each region to every other region [80].

Regional network properties were also calculated including *centrality*, *degree*, and *betweenness centrality*. *Centrality* represents the relative importance of a brain region within the network. *Degree* is the simplest measure of *centrality*. *Degree* is the number of regions connected to a region and regions with high *degree* are considered essential for maintaining global connectedness. *Betweenness centrality* refers to the fraction of shortest *paths* that pass through a region and regions with high *betweenness centrality* are considered critical for information flow. The *clustering coefficient* for each node was also computed, reflecting the fraction of a region's neighbor's that are also neighbors with each other and are thought to be key nodes for clusters or modules in the brain. Finally, *network hubs* were identified as regions whose *regional betweenness/degree* was 2 standard deviations greater than the average regional *betweenness/degree*. Hubs are considered important controllers of information flow and critical for efficient network communication.

Network parameters were quantified with respect to null-hypothesis networks having a random topology but sharing the same number of regions, connections, and *degree* (number of connections) distribution. To test for between-group differences in global and regional network measures, a non-parametric permutation test with 1000 repetitions was performed resulting in a permuted distribution of differences [60]. The p value for the group differences in regional measures was then calculated based on the percentile position of the group difference on the permuted distribution. We did not implement error control for multiple regions tested. Regional network measures were only compared at the minimum network density.

2.2.5. Data visualization—Pajek software (version 2.03) [36] was used to visualize the *betweenness* of structural brain network in IBS and HCs. A node represented each ROI, and

two regions with significant correlation (positive or negative) were linked by an edge. A Kamada–Kawai algorithm [67], a “spring embedding algorithm” was applied to create and optimize the structural network layout by minimizing variation in edge length [36].

3.1.0. Results

3.1.1. Sample Characteristics

Clinical and behavioral variables for IBS and HCs are shown in Tables 4 and 5. Patients had significantly higher levels of state and trait anxiety, symptoms of depression, and catastrophizing than HCs. Even though elevated, average levels of anxiety and depression symptoms were within the normal range. The sample was predominantly premenopausal 145 (72%), ranging in age from 18 to 52. Within groups, 90% HCs and 93% IBS were premenopausal. Four participants (2%) reported being perimenopausal (HC=3(3%), IBS=1(2%)), ages ranging from 35 to 50, and 9 (4%) reported being postmenopausal (age range, 48 to 64, HCs=6 (7%), IBS=3 (4%)). Forty-two (21%) females, ages ranging from 18 to 56 did not respond to the question. Of these 42 subjects, only 1 IBS patient was older than 55 years.

3.2.1. MRI Acquisition protocols and whole brain tissue classification

The 7 studies were comprised of 4 separate acquisition protocols, and the description of the acquisition protocols as well as the distribution of subjects and protocols across studies are described in Table 1 and 2. Linear contrasts analysis using GLM estimates comparing potential protocol differences in tissue classification across groups indicated no statistically significant differences in total GM or TBV between sites after adjusting p values to correct for number of contrasts performed. Linear contrasts indicated no protocol differences in total GM (q 's ranged from .11 to .94) or TBV (all q 's ranged from .71 to .93). We also found no indication of protocol*group interaction effects. Figure 3 depicts TBV and TGM by protocol and group.

3.2.2. Volumetric analysis comparing regions of interest between IBS and HCs

One subject failed in the LONI Pipeline workflow leaving 201 subjects available for the group analysis. Volumetric analysis demonstrated several highly significant moderate effect size *reductions* in regional GM volume in IBS patients compared to HCs, including bilateral superior frontal gyrus, bilateral insula, bilateral amygdala, bilateral hippocampus, bilateral middle orbital frontal gyrus, left cingulate, left gyrus rectus, brainstem, and left putamen (See Table 6, Figure 4). *Higher* GM volume was only seen in the left post-central gyrus (S1).

3.2.3. Effects of trait anxiety and early life events (ETI global score) on volumetric changes

Group differences were reexamined after controlling for trait anxiety and ETI score (See Table 6). Neither anxiety nor ETI global scores were found to be significant predictors based on uncorrected p values. However, when controlling for ETI global score, group differences were no longer significant for most regions except for the right amygdala and the L post central gyrus. These findings suggest a relationship between GM volume and ETI score. Group differences were generally found to be robust to the inclusion of trait anxiety as a covariate.

3.2.4. Correlations of volumetric changes with GI symptoms in IBS

Exploratory correlation analysis controlling for TBV found small effect size associations between higher abdominal pain reports and overall symptom severity and lower volumes in left inferior frontal gyrus ($r=-.26$, $p=.02$; $r=-.26$, $p=.02$), left middle orbital frontal gyrus ($r=-.28$, $p=.01$; $r=-.29$, $p=.01$), and left lateral orbital frontal gyrus ($r=-.31$, $p=.006$; $r=-.33$, $p=.004$). Higher volume in the left superior frontal gyrus ($r=-.26$, $p=.02$) was associated with more abdominal pain in IBS. Greater duration of IBS was negatively associated with right inferior frontal gyri ($r=-.26$, $p=.02$). Lower volumes in left insula was also associated with greater overall symptom severity ($r=-.26$, $p=.03$).

3.3.1. Network analysis

The *minimum density* threshold, ($D=.17$) was achieved by thresholding the interregional volumetric correlation matrix at $r=.32$ for IBS and $r=.25$ for HC. The thresholded interregional covariance matrices used to create volumetric networks are depicted in Figure 5.

Global organization—Both HC and IBS structural networks were considered small world networks as the *small-worldness* index was greater than 1 across the entire range of *densities*. (See Figure 6), No group differences were found for other measures of global and local network organization (*characteristic path length*, *clustering*, *modularity*, *efficiency*) across the range of *wiring costs* or at the *minimum density* (see Table 7).

Regional organization—At the *minimum density*, we performed group comparisons of several measures indicative of how much impact a particular brain region exerts on the whole brain structural network including normalized *degree*, normalized *clustering coefficient*, and normalized *betweenness*. In terms of regions which were considered essential for maintaining global connectedness, right cingulate (*degree* (D), $D_{HC}=4$, $D_{IBS}=16$, $p=.044$) and the right lateral orbital frontal gyrus ($D_{HC}=6$, $D_{IBS}=13$, $p=.045$) had significantly greater *degree* in IBS whereas the right angular gyrus ($D_{HC}=12$, $D_{IBS}=2$, $p=.042$), and the left cingulate gyrus ($D_{HC}=25$, $D_{IBS}=21$, $p=.048$) and the right fusiform gyrus ($D_{HC}=23$, $D_{IBS}=17$, $p=.041$) had significantly greater *degree* in HCs compare to IBS.

Brain regions at the intersection of many *paths* and therefore capable of controlling information are characterized by high regional *betweenness*. IBS compared to HCs showed significantly higher *betweenness* for the right cingulate gyrus (*betweenness* (B), $B_{HC}=4.7$, $B_{IBS}=96.7$, $p=.029$), and right thalamus ($B_{HC}=108.1$, $B_{IBS}=356.4$, $p=.020$). On the other hand, HCs showed significantly greater *betweenness* for the right inferior temporal gyrus ($B_{HC}=236$, $B_{IBS}=39.2$, $p=.010$), left cingulate ($B_{HC}=133.57$, $B_{IBS}=33.40$, $p=.036$), left ($B_{HC}=389.8$, $B_{IBS}=37.7$, $p=.020$) and right hippocampus ($B_{HC}=409.5$, $B_{IBS}=122.1$, $p=.040$).

In IBS compared to HC, the *clustering coefficient* for the left cingulate gyrus (*clustering coefficient* (C), $C_{HC}=.61$, $C_{IBS}=.75$, $p=.017$), right caudate ($C_{HC}=.67$, $C_{IBS}=.83$) and left hippocampus ($C_{HC}=.50$, $C_{IBS}=.74$, $p=.029$) was greater, indicating these regions are most densely connected with other regions and likely key for brain modules or clusters in IBS. In

HCs, the right middle temporal gyrus ($C_{HC}=1.0$, $C_{IBS}=.33$, $p=.039$) had a greater *clustering coefficient* compared to IBS.

Finally, *network hubs* were identified as regions whose *regional betweenness/degree* was 2 standard deviations greater than the average regional *betweenness/degree*. The average regional *degree* (SD) was $D_{HC}=11(8.1)$ and $D_{IBS}=11(7.4)$. The average *betweenness* for was $B_{HC}=97.16(104.2)$ and $B_{IBS}=88.8(102.4)$. Network hub analysis indicated that the right parahippocampal gyrus, ($B_{HC}=289.6$, $B_{IBS}=259.6$) and left lingual gyrus ($B_{HC}=311.4$, $B_{IBS}=460.0$) were important *hubs* in both groups. For IBS, additional *hubs* included brainstem ($B=384.3$), right thalamus ($B=356.4$), left inferior frontal gyrus ($D=26$) and left insular gyrus ($D_{IBS}=28$). For HCs, left precuneus ($B=366.1$) and bilateral hippocampus ($B_{right}=389.1$, $B_{left}=409.5$) were considered *hub* regions. The right insular gyrus ($D_{IBS}=27$) was also identified as a *hub* in HCs and the right hippocampus ($B=409.5$) was identified as a *hub* in IBS. Figure 7 depicts the IBS and HC structural networks based on within group *betweenness* metrics for each region.

4.1.1. Discussion

In the current study, we compared regional GM volume from 82 well phenotyped, predominantly premenopausal female IBS and 119 HC subjects, by combining structural imaging data from multiple studies performed at UCLA. We found: 1) Lower GM volume were identified in insula, cingulate, amygdala, hippocampus, putamen and frontal regions, while greater GMV was observed in S1 for IBS compared to HC. 2) Many of the differences were accounted for by a history of EALs but not trait anxiety. 3) Similarities and differences between the two groups in global and regional network characteristics based on regional GM volume changes were observed. To our knowledge, this is the first report of structural brain network alterations in IBS, and the largest analysis of regional GM volume changes for any pain disorder.

4.2.0. Novelty of combining and analyzing data from individual studies

We demonstrated widespread alterations in GM volume in a large number of IBS patients from 7 individual studies, and changes in identified regions were largely consistent with those reported in previous studies. Aggregating data across multiple studies and sites through mega-analyses has accelerated progress in mapping brain structure and function and improved on the limitations of current meta-analytic efforts by increasing statistical power, reliability of findings, representativeness of samples, and the ability to study the causes of variability across various experiments [29]. Although between-study factors may be a source of variability, results that generalize over multiple studies are considered more reliable and less likely to be related to the characteristics of a single study's design [29].

4.3.0. Significant GM volume changes between IBS and HCs

Compared to HCs, IBS showed moderate effect size *reductions* (Cohen's $d=.30$ to $.61$) in a range of brain regions including bilateral insula, bilateral superior frontal gyrus, bilateral middle orbital frontal gyrus, bilateral hippocampus, bilateral amygdala, left cingulate gyrus, left gyrus rectus, left putamen and brainstem. In contrast, *higher* GM volume in IBS was

only observed for S1. The identified regions with lower GM volumes (including insula, amygdala, cingulate, hippocampus, brainstem, prefrontal modulatory regions and the basal ganglia) are similar to previously reported GM [12; 35; 116] and white matter [25] changes in smaller samples of IBS patients, in some studies with other chronic pain conditions including chronic lower back pain, fibromyalgia, migraine, chronic tension type headache, migraine, chronic facial pain, chronic pain in hip osteoarthritis and chronic regional pain syndrome [89], and patients with affective disorders [13; 63; 74]. However, significant differences to previously published studies in IBS patient populations were also observed. In particular the studies differed in brain regions that showed *higher* GM, with one showing higher GM volume in the hypothalamus [12], and the other, OFG and a trend in posterior INS/S2 cortex [116]. These differences may be due to differences in patient characteristics, use of different statistical algorithms and templates, increased power in the present study to detect moderate effect size differences, rigorous error control applied in the present study, and decreases in variability in the sampling mean estimates afforded by increased sample size.

The current study demonstrates significantly higher GM volume in IBS in S1, a brain region involved in sensory discriminative processing of both noxious and innocuous stimuli [68–70]. GM differences in S1 have been reported both in different chronic pain conditions [33; 38; 53; 54; 71; 94] and in HCs with greater somatic pain sensitivity [44]. For example, in HCs without any pain history a positive correlation between CT in S1 and pain and temperature sensitivity, and a negative correlation of temperature sensitivity with CT in the anterior midcingulate cortex has been reported [44]. Also, in HCs GM increases in response to repetitive noxious stimulation in S1 and ACC have recently been reported [129]. It has been suggested that the critical factor for S1 to undergo functional and structural reorganization maybe the presence of constant sensory input to this brain region [53]. While the basis for such ongoing input to S1 in IBS patients remains unknown, such signals may arise from gut microbial factors [96] from mucosal immune activation [119] or from increased spinothalamic input secondary to alterations in descending pain modulation systems [21]. Consistent with extensive alterations in the somatosensory system are symptom reports [23], and results from quantitative pain testing [104; 125] showing widespread somatic hyperalgesia in IBS patients, including heat pain stimuli. In addition, a recent DTI study has identified widespread microstructural changes in sensory processing and modulation areas of the brain [43].

The mechanisms underlying the observed GM alterations remain to be determined, even though various molecular mechanisms have been proposed [10; 82; 109]. Ultimately, it is unclear whether the observed changes are a consequence of having a chronic pain disorder [34; 89], or if they are underlying, possibly genetically/epigenetically determined risk factors. The fact that lower prefrontal, cingulate, insula, left insula, putamen and hippocampal GM volumes were no longer observed after correction for EALs suggests that these changes may not be specific for IBS per se, and are more related to EALs often reported by IBS patients, and other patients with persistent pain disorders [3; 14; 101]. Lower GM volumes in hippocampus, amygdala, PFC, anterior cingulate and basal ganglia have previously been reported in subjects with a history of EAL [22; 28; 56; 65]. Such EAL-

related structural brain changes may be the consequence of epigenetic modifications of gene expression, including glucocorticoid receptor methylation and resulting chronically elevated plasma cortisol levels [22]. The small correlations identified between frontal brain regions and abdominal pain, fronto-insular regions and symptom severity, and between the left inferior frontal gyrus and symptom duration suggest possible correlations between the observed structural changes and IBS symptoms, but larger samples are needed to replicate these exploratory observations.

4.4.0. Network analyses

No statistically significant group differences were found for network indices of global or local efficiency of information transfer between regions. Consistent with previous studies examining GM morphometry in HCs [7; 58] and migraine patients [85], the global organization of structural networks based on GM volume in HC subjects as well as IBS showed small world properties, which are thought to provide the optimal balance between network segregation and integration resulting in economical brain functioning that minimizes wiring cost and supports dynamic complexity [7; 19].

With regard to regional network properties, several group differences were observed potentially reflecting disease-related alterations in brain regions that are critical in facilitating global integrative processes and communication. Compared to HCs, the right cingulate gyrus and right thalamus, were found to be more critical for controlling information in IBS. This greater *betweenness* has also been reported for anterior cingulate, midcingulate and thalamic GM volumes in female migraine patients compared to HCs [85]. This lends support to the view that other often comorbid pain conditions may have similar underlying brain network alterations which affect the processing and modulation of sensory information [32; 72; 126].

The regions identified as unique hubs in IBS are regions shown in functional MRI studies to be involved in endogenous pain modulation and central sensory amplification including left inferior frontal cortex, left insular cortex, right thalamus and brainstem [137]. While the observed alterations in regional topology provide strong evidence for extensive structural reorganization of cortical and subcortical regions previously implicated in altered brain responses to visceral pain stimuli and their expectation [55; 87; 133], the current study does not allow us to implicate specific physiological or molecular mechanisms underlying these changes.

4.5.0. Study limitations

Our method of data aggregation is similar to other recent efforts to gain power by combining multi-site data [11]. Although the current study was adequately powered to detect medium effect size volumetric differences, small effect size differences cannot be ruled out. Although, we found no differences in TGM or TBV by acquisition protocol, we cannot rule out variance due to acquisition parameters. Due to the nature of the experimental design, variability accounted for by specific and nonspecific study effects and acquisition protocols is confounded and cannot be separated. Unfortunately, the size of some of the LBPA 40 atlas template regions limited our ability to parse out specific subregions of the insula,

cingulate cortex, and prefrontal cortex [19]. With regard to the network analysis, inter-regional volumetric connectivity does not necessarily reflect anatomical (i.e., white matter tracts) or functional connectivity, although moderate approximations have been reported [52; 64; 81]. Our findings about basic network properties and some specific alterations are consistent with previously reported regional structural and functional alterations,[34] including alterations in network properties in chronic pain conditions[85], and suggests structural alterations in brain networks involved in sensory processing and modulation. However, the correlation of the observed network alterations based on grey matter changes with structural and functional network alterations based on other imaging and analysis modalities (including probabilistic tractography and resting state networks), as well as the clinical consequences of such network alterations remain to be determined [16].

4.6.0. Summary and conclusions

The observed changes (increases and decreases) in GM volume and alterations in regional network properties identified in this study may reflect different pathophysiological components of the disease processes underlying IBS symptoms, including increased sensitivity to somatic and visceral stimuli (higher GM volumes in S1), associated increase in emotional arousal (lower GM in hippocampus in IBS) and other chronic pain related mechanisms (lower GM in insula and cingulate cortices, differences in insula, cingulate, thalamus and brain stem network properties). Future studies in large well phenotyped samples of patients, as well as in animal models of chronic pain will be required to address these hypotheses.

Supplementary Material

Refer to Web version on PubMed Central for supplementary material.

Acknowledgments

This work was funded in part by the National Institutes of Health through Center for Neurobiology (CNS) Grants: K08 DK071626, R03 DK084169 (JSL), K23DK073451, R01 AT007137(KT), P50 DK064539 (EAM), R01 DK048351 (EAM), and LONI Grants: P41-EB015922, U24-RR025736, U24-RR026057, R01MH094343, U01 MH093765. We are also indebted to Cathy Liu for database management and graphic support (P30 DK041301) and the members of the Laboratory of Neuro Imaging (LONI) for support, module definitions and workflow protocol designs.

Abbreviations

IBS	Irritable bowel syndrome
HCS	healthy controls
GM	gray matter
VBM	voxel-based morphometry
CT	cortical thickness
ROI	region of interest
S1	somatosensory cortex

ACC	anterior cingulate cortex
mOFG	middle orbitofrontal gyrus
PFC	prefrontal cortex
HPA	hypothalamic pituitary adrenal
LONI	Laboratory of Neuroimaging
GI	gastroenterology
EALs	early adverse life events
ETI	Early Life Trauma Inventory
STAI	State Trait Anxiety Inventory
HAD	Hospital Anxiety and Depression Scale
CSQ	Coping Strategies Questionnaire
PHQ	Patient Health Questionnaire
BSQ	Bowel Symptoms Questionnaire
GLM	general linear model
L	left
R	right
C	clustering coefficient
D	degree
B	betweenness

References

1. Achard S, Bullmore E. Efficiency and cost of economical brain functional networks. *PLoS computational biology*. 2007; 3(2):e17. [PubMed: 17274684]
2. Agostini A, Benuzzi F, Filipini N, Bertani A, Scarcelli A, Farinelli V, Marchetta C, Calabrese C, Rizzello F, Gionchetti P, Ercolani M, Campieri M, Nichelli P. New insights into the brain involvement in patients with Crohn's disease: a voxel-based morphometry study. *Neurogastroenterology and motility : the official journal of the European Gastrointestinal Motility Society*. 2012
3. Anda R, Tietjen G, Schulman E, Felitti V, Croft J. Adverse childhood experiences and frequent headaches in adults. *Headache*. 2010; 50(9):1473–1481. [PubMed: 20958295]
4. Apkarian AV, Sosa Y, Sonty S, Levy RM, Harden RN, Parrish TB, Gitelman DR. Chronic back pain is associated with decreased prefrontal and thalamic gray matter density. *The Journal of neuroscience : the official journal of the Society for Neuroscience*. 2004; 24(46):10410–10415. [PubMed: 15548656]
5. As-Sanie S, Harris RE, Napadow V, Kim J, Neshewat G, Kairys A, Williams D, Clauw DJ, Schmidt-Wilcke T. Changes in regional gray matter volume in women with chronic pelvic pain: a voxel-based morphometry study. *Pain*. 2012; 153(5):1006–1014. [PubMed: 22387096]
6. Baliki MN, Schnitzer TJ, Bauer WR, Apkarian AV. Brain Morphological Signatures for Chronic Pain. *PloS one*. 2011; 6(10)

7. Bassett DS, Bullmore E. Small-world brain networks. *The Neuroscientist : a review journal bringing neurobiology, neurology and psychiatry*. 2006; 12(6):512–523.
8. Bassett DS, Bullmore E, Verchinski BA, Mattay VS, Weinberger DR, Meyer-Lindenberg A. Hierarchical organization of human cortical networks in health and schizophrenia. *The Journal of neuroscience : the official journal of the Society for Neuroscience*. 2008; 28(37):9239–9248. [PubMed: 18784304]
9. Bassett DS, Bullmore ET. Human brain networks in health and disease. *Curr Opin Neurol*. 2009; 22(4):340–347. [PubMed: 19494774]
10. Biedermann S, Fuss J, Zheng L, Sartorius A, Falfan-Melgoza C, Demirakca T, Gass P, Ende G, Weber-Fahr W. In vivo voxel based morphometry: Detection of increased hippocampal volume and decreased glutamate levels in exercising mice. *NeuroImage*. 2012; 61(4):1206–1212. [PubMed: 22521257]
11. Biswal BB, Mennes M, Zuo XN, Gohel S, Kelly C, Smith SM, Beckmann CF, Adelstein JS, Buckner RL, Colcombe S, Dogonowski AM, Ernst M, Fair D, Hampson M, Hoptman MJ, Hyde JS, Kiviniemi VJ, Kotter R, Li SJ, Lin CP, Lowe MJ, Mackay C, Madden DJ, Madsen KH, Margulies DS, Mayberg HS, McMahon K, Monk CS, Mostofsky SH, Nagel BJ, Pekar JJ, Peltier SJ, Petersen SE, Riedl V, Rombouts SA, Rypma B, Schlaggar BL, Schmidt S, Seidler RD, Siegle GJ, Sorg C, Teng GJ, Veijola J, Villringer A, Walter M, Wang L, Weng XC, Whitfield-Gabrieli S, Williamson P, Windischberger C, Zang YF, Zhang HY, Castellanos FX, Milham MP. Toward discovery science of human brain function. *Proceedings of the National Academy of Sciences of the United States of America*. 2010; 107(10):4734–4739. [PubMed: 20176931]
12. Blankstein U, Chen J, Diamant NE, Davis KD. Altered brain structure in irritable bowel syndrome: potential contributions of pre-existing and disease-driven factors. *Gastroenterology*. 2010; 138(5):1783–1789. [PubMed: 20045701]
13. Bora E, Fornito A, Pantelis C, Yucel M. Gray matter abnormalities in Major Depressive Disorder: A meta-analysis of voxel based morphometry studies. *J Affect Disorders*. 2012; 138(1–2):9–18. [PubMed: 21511342]
14. Bradford K, Shih W, Videlock EJ, Presson AP, Naliboff BD, Mayer EA, Chang L. Association between early adverse life events and irritable bowel syndrome. *Clinical gastroenterology and hepatology : the official clinical practice journal of the American Gastroenterological Association*. 2012; 10(4):385–390. e381–383. [PubMed: 22178460]
15. Bremner JD, Bolus R, Mayer EA. Psychometric properties of the Early Trauma Inventory-Self Report. *J Nerv Ment Dis*. 2007; 195(3):211–218. [PubMed: 17468680]
16. Brown JA, Rudie JD, Bandrowski A, Van Horn JD, Bookheimer SY. The UCLA multimodal connectivity database: a web-based platform for brain connectivity matrix sharing and analysis. *Frontiers in neuroinformatics*. 2012; 6:28. [PubMed: 23226127]
17. Bullmore E, Sporns O. Complex brain networks: graph theoretical analysis of structural and functional systems. *Nature reviews Neuroscience*. 2009; 10(3):186–198.
18. Bullmore E, Sporns O. The economy of brain network organization. *Nature reviews Neuroscience*. 2012; 13(5):336–349.
19. Bullmore ET, Bassett DS. Brain graphs: graphical models of the human brain connectome. *Annual review of clinical psychology*. 2011; 7:113–140.
20. Burgmer M, Gaubitz M, Konrad C, Wrenger M, Hilgart S, Heuft G, Pfliederer B. Decreased gray matter volumes in the cingulo-frontal cortex and the amygdala in patients with fibromyalgia. *Psychosomatic medicine*. 2009; 71(5):566–573. [PubMed: 19414621]
21. Bushnell MC, Ceko M, Low LA. Cognitive and emotional control of pain and its disruption in chronic pain. *Nature reviews Neuroscience*. 2013; 14(7):502–511.
22. Carrion VG, Wong SS. Can traumatic stress alter the brain? Understanding the implications of early trauma on brain development and learning. *The Journal of adolescent health : official publication of the Society for Adolescent Medicine*. 2012; 51(2 Suppl):S23–28. [PubMed: 22794529]
23. Chang L, Mayer EA, Johnson T, FitzGerald LZ, Naliboff B. Differences in somatic perception in female patients with irritable bowel syndrome with and without fibromyalgia. *Pain*. 2000; 84(2–3):297–307. [PubMed: 10666535]

24. Chen CH, Gutierrez ED, Thompson W, Panizzon MS, Jernigan TL, Eyler LT, Fennema-Notestine C, Jak AJ, Neale MC, Franz CE, Lyons MJ, Grant MD, Fischl B, Seidman LJ, Tsuang MT, Kremen WS, Dale AM. Hierarchical genetic organization of human cortical surface area. *Science*. 2012; 335(6076):1634–1636. [PubMed: 22461613]
25. Chen JYW, Blankstein U, Diamant NE, Davis KD. White matter abnormalities in irritable bowel syndrome and relation to individual factors. *Brain research*. 2011; 1392:121–131. [PubMed: 21466788]
26. Chen ZJ, He Y, Rosa-Neto P, Germann J, Evans AC. Revealing modular architecture of human brain structural networks by using cortical thickness from MRI. *Cereb Cortex*. 2008; 18(10):2374–2381. [PubMed: 18267952]
27. Cohen MX, Lombardo MV, Blumenfeld RS. Covariance-based subdivision of the human striatum using T1-weighted MRI. *Eur J Neurosci*. 2008; 27(6):1534–1546. [PubMed: 18364027]
28. Cohen RA, Grieve S, Hoth KF, Paul RH, Sweet L, Tate D, Gunstad J, Stroud L, McCaffery J, Hitsman B, Niaura R, Clark CR, McFarlane A, Bryant R, Gordon E, Williams LM. Early life stress and morphometry of the adult anterior cingulate cortex and caudate nuclei. *Biological psychiatry*. 2006; 59(10):975–982. [PubMed: 16616722]
29. Costafreda SG. Pooling FMRI data: meta-analysis, mega-analysis and multi-center studies. *Frontiers in neuroinformatics*. 2009; 3:33. [PubMed: 19826498]
30. Craig AD. Interoception: the sense of the physiological condition of the body. *Current opinion in neurobiology*. 2003; 13(4):500–505. [PubMed: 12965300]
31. Craig AD. A new view of pain as a homeostatic emotion. *Trends in neurosciences*. 2003; 26(6):303–307. [PubMed: 12798599]
32. Critchley HD, Nagai Y, Gray MA, Mathias CJ. Dissecting axes of autonomic control in humans: Insights from neuroimaging. *Autonomic neuroscience : basic & clinical*. 2011; 161(1–2):34–42. [PubMed: 20926356]
33. DaSilva AF, Granziera C, Snyder J, Hadjikhani N. Thickening in the somatosensory cortex of patients with migraine. *Neurology*. 2007; 69(21):1990–1995. [PubMed: 18025393]
34. Davis KD, Moayedi M. Central mechanisms of pain revealed through functional and structural MRI. *Journal of neuroimmune pharmacology : the official journal of the Society on NeuroImmune Pharmacology*. 2013; 8(3):518–534. [PubMed: 22825710]
35. Davis KD, Pope G, Chen J, Kwan CL, Crawley AP, Diamant NE. Cortical thinning in IBS: implications for homeostatic, attention, and pain processing. *Neurology*. 2008; 70(2):153–154. [PubMed: 17959767]
36. De Nooy, W.; Mrvar, A.; Batagelj, V. *Exploratory Social Network Analysis with Pajek*. Cambridge: Cambridge University Press; 2011.
37. Desikan RS, Segonne F, Fischl B, Quinn BT, Dickerson BC, Blacker D, Buckner RL, Dale AM, Maguire RP, Hyman BT, Albert MS, Killiany RJ. An automated labeling system for subdividing the human cerebral cortex on MRI scans into gyral based regions of interest. *NeuroImage*. 2006; 31(3):968–980. [PubMed: 16530430]
38. Desouza DD, Moayedi M, Chen DQ, Davis KD, Hodaie M. Sensorimotor and Pain Modulation Brain Abnormalities in Trigeminal Neuralgia: A Paroxysmal, Sensory-Triggered Neuropathic Pain. *PloS one*. 2013; 8(6):e66340. [PubMed: 23823184]
39. Dinov I, Lozev K, Petrosyan P, Liu Z, Eggert P, Pierce J, Zamanyan A, Chakrapani S, Van Horn J, Parker D, Magsipoc R, Leung K, Gutman B, Woods R, Toga A. Neuroimaging Study Designs, Computational Analyses and Data Provenance Using the LONI Pipeline. *PLoS ONE*. 2010; 5(9):e13070. doi:13010.11371/journal.pone.0013070. [PubMed: 20927408]
40. Dinov I, Lozev K, Petrosyan P, Liu Z, Eggert P, Pierce J, Zamanyan A, Chakrapani S, Van Horn J, Parker DS, Magsipoc R, Leung K, Gutman B, Woods R, Toga A. Neuroimaging study designs, computational analyses and data provenance using the LONI pipeline. *PloS one*. 2010; 5(9)
41. Dinov I, Torri F, Macchiardi F, Petrosyan P, Liu Z, Zamanyan A, Eggert P, Pierce J, Genco A, Knowles J, Clark A, Van Horn J, Ames J, Kesselman C, Toga A. Applications of the Pipeline Environment for Visual Informatics and Genomics Computations. *BMC Bioinformatics*. 2011; 12(1):304. [PubMed: 21791102]

42. Dinov ID, Van Horn JD, Lozev KM, Magsipoc R, Petrosyan P, Liu Z, Mackenzie-Graham A, Eggert P, Parker DS, Toga AW. Efficient, Distributed and Interactive Neuroimaging Data Analysis Using the LONI Pipeline. *Frontiers in neuroinformatics*. 2009; 3:22. [PubMed: 19649168]
43. Ellingson BM, Mayer E, Harris RJ, Ashe-McNally C, Naliboff BD, Labus JS, Tillisch K. Diffusion tensor imaging detects microstructural reorganization in the brain associated with chronic irritable bowel syndrome. *Pain*. 2013
44. Erpelding N, Moayed M, Davis KD. Cortical thickness correlates of pain and temperature sensitivity. *Pain*. 2012; 153(8):1602–1609. [PubMed: 22516588]
45. Evans AC. Networks of anatomical covariance. *NeuroImage*. 2013; 80:489–504. [PubMed: 23711536]
46. Ferrer I, Alcantara S, Ballabriga J, Olive M, Blanco R, Rivera R, Carmona M, Berruezo M, Pitarch S, Planas AM. Transforming growth factor-alpha (TGF-alpha) and epidermal growth factor-receptor (EGF-R) immunoreactivity in normal and pathologic brain. *Progress in neurobiology*. 1996; 49(2):99–123. [PubMed: 8844822]
47. Ferrer I, Blanco R, Carulla M, Condom M, Alcantara S, Olive M, Planas A. Transforming growth factor-alpha immunoreactivity in the developing and adult brain. *Neuroscience*. 1995; 66(1):189–199. [PubMed: 7637868]
48. Fischl B, Dale AM. Measuring the thickness of the human cerebral cortex from magnetic resonance images. *Proceedings of the National Academy of Sciences of the United States of America*. 2000; 97(20):11050–11055. [PubMed: 10984517]
49. Frokjaer JB, Olesen SS, Gram M, Yavarian Y, Bouwense SAW, Wilder-Smith OHG, Drewes AM. Altered brain microstructure assessed by diffusion tensor imaging in patients with chronic pancreatitis. *Gut*. 2011; 60(11):1554–1562. [PubMed: 21610272]
50. Geha PY, Baliki MN, Harden RN, Bauer WR, Parrish TB, Apkarian AV. The brain in chronic CRPS pain: abnormal gray-white matter interactions in emotional and autonomic regions. *Neuron*. 2008; 60(4):570–581. [PubMed: 19038215]
51. Gerstner G, Ichesco E, Quintero A, Schmidt-Wilcke T. Changes in regional gray and white matter volume in patients with myofascial-type temporomandibular disorders: a voxel-based morphometry study. *Journal of orofacial pain*. 2011; 25(2):99–106. [PubMed: 21528116]
52. Gong G, He Y, Chen ZJ, Evans AC. Convergence and divergence of thickness correlations with diffusion connections across the human cerebral cortex. *NeuroImage*. 2012; 59(2):1239–1248. [PubMed: 21884805]
53. Gustin SM, Peck CC, Cheney LB, Macey PM, Murray GM, Henderson LA. Pain and Plasticity: Is Chronic Pain Always Associated with Somatosensory Cortex Activity and Reorganization? *Journal of Neuroscience*. 2012; 32(43):14874–14884. [PubMed: 23100410]
54. Gustin SM, Peck CC, Wilcox SL, Nash PG, Murray GM, Henderson LA. Different pain, different brain: thalamic anatomy in neuropathic and non-neuropathic chronic pain syndromes. *The Journal of neuroscience : the official journal of the Society for Neuroscience*. 2011; 31(16):5956–5964. [PubMed: 21508220]
55. Hall GBC, Kamath MV, Collins S, Ganguli S, Spaziani R, Miranda KL, Bayati A, Bienenstock J. Heightened central affective response to visceral sensations of pain and discomfort in IBS. *Neurogastroent Motil*. 2010; 22(3)
56. Hanson JL, Chung MK, Avants BB, Shirtcliff EA, Gee JC, Davidson RJ, Pollak SD. Early stress is associated with alterations in the orbitofrontal cortex: a tensor-based morphometry investigation of brain structure and behavioral risk. *The Journal of neuroscience : the official journal of the Society for Neuroscience*. 2010; 30(22):7466–7472. [PubMed: 20519521]
57. He Y, Chen Z, Evans A. Structural insights into aberrant topological patterns of large-scale cortical networks in Alzheimer's disease. *The Journal of neuroscience : the official journal of the Society for Neuroscience*. 2008; 28(18):4756–4766. [PubMed: 18448652]
58. He Y, Chen ZJ, Evans AC. Small-world anatomical networks in the human brain revealed by cortical thickness from MRI. *Cereb Cortex*. 2007; 17(10):2407–2419. [PubMed: 17204824]
59. He Y, Evans A. Graph theoretical modeling of brain connectivity. *Curr Opin Neurol*. 2010; 23(4): 341–350. [PubMed: 20581686]

60. Hosseini SM, Hoefft F, Kesler SR. GAT: A Graph-Theoretical Analysis Toolbox for Analyzing Between-Group Differences in Large-Scale Structural and Functional Brain Networks. *PloS one*. 2012; 7(7):e40709. [PubMed: 22808240]
61. Hosseini SM, Koovakkattu D, Kesler SR. Altered small-world properties of gray matter networks in breast cancer. *BMC neurology*. 2012; 12:28. [PubMed: 22632066]
62. Hubbard CS, Labus JS, Bueller J, Stains J, Suyenobu B, Dukes GE, Kelleher DL, Tillisch K, Naliboff BD, Mayer EA. Corticotropin-releasing factor receptor 1 antagonist alters regional activation and effective connectivity in an emotional-arousal circuit during expectation of abdominal pain. *The Journal of neuroscience : the official journal of the Society for Neuroscience*. 2011; 31(35):12491–12500. [PubMed: 21880911]
63. Inkster B, Rao AW, Ridler K, Nichols TE, Saemann PG, Auer DP, Holsboer F, Tozzi F, Muglia P, Merlo-Pich E, Matthews PM. Structural Brain Changes in Patients with Recurrent Major Depressive Disorder Presenting with Anxiety Symptoms. *J Neuroimaging*. 2011; 21(4):375–382. [PubMed: 20977527]
64. Irimia A, Van Horn JD. The structural, connectomic and network covariance of the human brain. *NeuroImage*. 2012; 66C:489–499. [PubMed: 23116816]
65. Jackowski A, Perera TD, Abdallah CG, Garrido G, Tang CY, Martinez J, Mathew SJ, Gorman JM, Rosenblum LA, Smith EL, Dwork AJ, Shungu DC, Kaffman A, Gelernter J, Coplan JD, Kaufman J. Early-life stress, corpus callosum development, hippocampal volumetrics, and anxious behavior in male nonhuman primates. *Psychiatry research*. 2011; 192(1):37–44. [PubMed: 21377844]
66. Jenkinson M, Beckmann CF, Behrens TE, Woolrich MW, Smith SM. *Fsl. NeuroImage*. 2012; 62(2):782–790.
67. Kamada T, Kawai S. An algorithm for drawing general undirected graphs. *Information Processing Letters*. 1989; 31(1):7–15.
68. Kenshalo DR, Chudler EH, Anton F, Dubner R. Si Nociceptive Neurons Participate in the Encoding Process by Which Monkeys Perceive the Intensity of Noxious Thermal-Stimulation. *Brain research*. 1988; 454(1–2):378–382. [PubMed: 3409021]
69. Kenshalo DR, Isensee O. Responses of Primate Si Cortical-Neurons to Noxious Stimuli. *Journal of neurophysiology*. 1983; 50(6):1479–1496. [PubMed: 6663338]
70. Kenshalo DR, Iwata K, Sholas M, Thomas DA. Response properties and organization of nociceptive neurons in area I of monkey primary somatosensory cortex. *Journal of neurophysiology*. 2000; 84(2):719–729. [PubMed: 10938299]
71. Kim JH, Suh SI, Seol HY, Oh K, Seo WK, Yu SW, Park KW, Koh SB. Regional grey matter changes in patients with migraine: a voxel-based morphometry study. *Cephalalgia : an international journal of headache*. 2008; 28(6):598–604. [PubMed: 18422725]
72. Kim S, Chang L. Overlap between functional GI disorders and other functional syndromes: what are the underlying mechanisms? *Neurogastroenterology and motility : the official journal of the European Gastrointestinal Motility Society*. 2012; 24(10):895–913. [PubMed: 22863120]
73. Kroenke K, Spitzer RL, Williams JB. The PHQ-15: validity of a new measure for evaluating the severity of somatic symptoms. *Psychosomatic medicine*. 2002; 64(2):258–266. [PubMed: 11914441]
74. Kroes MCW, Rugg MD, Whalley MG, Brewin CR. Structural brain abnormalities common to posttraumatic stress disorder and depression. *J Psychiatr Neurosci*. 2011; 36(4):256–265.
75. Kuchinad A, Schweinhardt P, Seminowicz DA, Wood PB, Chizh BA, Bushnell MC. Accelerated brain gray matter loss in fibromyalgia patients: premature aging of the brain? *The Journal of neuroscience : the official journal of the Society for Neuroscience*. 2007; 27(15):4004–4007. [PubMed: 17428976]
76. Kwan CL, Diamant NE, Pope G, Mikula K, Mikulis DJ, Davis KD. Abnormal forebrain activity in functional bowel disorder patients with chronic pain. *Neurology*. 2005; 65(8):1268–1277. [PubMed: 16247056]
77. Labus JS, Mayer EA, Jarcho J, Kilpatrick LA, Kilkens TO, Evers EA, Backes WH, Brummer RJ, van Nieuwenhoven MA. Acute tryptophan depletion alters the effective connectivity of emotional arousal circuitry during visceral stimuli in healthy women. *Gut*. 2011; 60(9):1196–1203. [PubMed: 21402618]

78. Labus JS, Naliboff BD, Berman SM, Suyenobu B, Vianna EP, Tillisch K, Mayer EA. Brain networks underlying perceptual habituation to repeated aversive visceral stimuli in patients with irritable bowel syndrome. *NeuroImage*. 2009; 47(3):952–960. [PubMed: 19501173]
79. Labus JS, Naliboff BN, Fallon J, Berman SM, Suyenobu B, Bueller JA, Mandelkern M, Mayer EA. Sex differences in brain activity during aversive visceral stimulation and its expectation in patients with chronic abdominal pain: a network analysis. *NeuroImage*. 2008; 41(3):1032–1043. [PubMed: 18450481]
80. Latora V, Marchiori M. Efficient behavior of small-world networks. *Phys Rev Lett*. 2001; 87(19)
81. Lerch JP, Worsley K, Shaw WP, Greenstein DK, Lenroot RK, Giedd J, Evans AC. Mapping anatomical correlations across cerebral cortex (MACACC) using cortical thickness from MRI. *NeuroImage*. 2006; 31(3):993–1003. [PubMed: 16624590]
82. Lerch JP, Yiu AP, Martinez-Canabal A, Pekar T, Bohbot VD, Frankland PW, Henkelman RM, Josselyn SA, Sled JG. Maze training in mice induces MRI-detectable brain shape changes specific to the type of learning. *NeuroImage*. 2011; 54(3):2086–2095. [PubMed: 20932918]
83. Leung, K. Principal Ranking Meta-Algorithms. University of California, Los Angeles: University of California, Los Angeles; 2010.
84. Leung, K.; Parker, DS.; Cunha, A.; Hojatkishimi, C.; Dinov, I.; Toga, A. Scientific and Statistical Database management. Vol. 5069. Berlin Heidelberg: Springer-Verlag; 2008. IRMA:An image registration algorithm; p. 612-617.
85. Liu J, Zhao L, Li G, Xiong S, Nan J, Li J, Yuan K, von Deneen KM, Liang F, Qin W, Tian J. Hierarchical alteration of brain structural and functional networks in female migraine sufferers. *PLoS one*. 2012; 7(12):e51250. [PubMed: 23227257]
86. Longstreth, GL.; Thompson, WG.; Chey, WD.; Houghton, LA.; Mearin, F.; Spiller, RC. Functional bowel disorders. In: Drossman, DA.; Corazziari, E.; Delvaux, M.; Spiller, RC.; Talley, NJ.; Thompson, WG.; Whitehead, WE., editors. Rome III: The functional gastrointestinal disorders. McLean, VA: Degnon Associates, Inc; 2006.
87. Lowen MB, Mayer EA, Sjöberg M, Tillisch K, Naliboff B, Labus J, Lundberg P, Strom M, Engstrom M, Walter SA. Effect of hypnotherapy and educational intervention on brain response to visceral stimulus in the irritable bowel syndrome. *Alimentary pharmacology & therapeutics*. 2013; 37(12):1184–1197. [PubMed: 23617618]
88. May A. Chronic pain may change the structure of the brain. *Pain*. 2008; 137(1):7–15. [PubMed: 18410991]
89. May A. Structural brain imaging: a window into chronic pain. *The Neuroscientist : a review journal bringing neurobiology, neurology and psychiatry*. 2011; 17(2):209–220.
90. Mayer EA, Berman S, Suyenobu B, Labus J, Mandelkern MA, Naliboff BD, Chang L. Differences in brain responses to visceral pain between patients with irritable bowel syndrome and ulcerative colitis. *Pain*. 2005; 115(3):398–409. [PubMed: 15911167]
91. Mayer EA, Naliboff BD, Craig AD. Neuroimaging of the brain-gut axis: from basic understanding to treatment of functional GI disorders. *Gastroenterology*. 2006; 131(6):1925–1942. [PubMed: 17188960]
92. Mechelli A, Friston KJ, Frackowiak RS, Price CJ. Structural covariance in the human cortex. *The Journal of neuroscience : the official journal of the Society for Neuroscience*. 2005; 25(36):8303–8310. [PubMed: 16148238]
93. Meunier D, Lambiotte R, Bullmore ET. Modular and hierarchically modular organization of brain networks. *Frontiers in neuroscience*. 2010; 4:200. [PubMed: 21151783]
94. Moayed M, Weissman-Fogel I, Crawley AP, Goldberg MB, Freeman BV, Tenenbaum HC, Davis KD. Contribution of chronic pain and neuroticism to abnormal forebrain gray matter in patients with temporomandibular disorder. *NeuroImage*. 2011; 55(1):277–286. [PubMed: 21156210]
95. Moayed M, Weissman-Fogel I, Salomons TV, Crawley AP, Goldberg MB, Freeman BV, Tenenbaum HC, Davis KD. Abnormal gray matter aging in chronic pain patients. *Brain research*. 2012; 1456:82–93. [PubMed: 22503149]
96. Modi SR, Lee HH, Spina CS, Collins JJ. Antibiotic treatment expands the resistance reservoir and ecological network of the phage metagenome. *Nature*. 2013

97. Mordasini L, Weisstanner C, Rummel C, Thalmann GN, Verma RK, Wiest R, Kessler TM. Chronic Pelvic Pain Syndrome in Men is Associated with Reduction of Relative Gray Matter Volume in the Anterior Cingulate Cortex Compared to Healthy Controls. *Journal of Urology*. 2012; 188(6):2233–2237. [PubMed: 23083652]
98. Munakata J, Naliboff B, Harraf F, Kodner A, Lembo T, Chang L, Silverman DH, Mayer EA. Repetitive sigmoid stimulation induces rectal hyperalgesia in patients with irritable bowel syndrome. *Gastroenterology*. 1997; 112(1):55–63. [PubMed: 8978343]
99. Mutso AA, Radzicki D, Baliki MN, Huang L, Banisadr G, Centeno MV, Radulovic J, Martina M, Miller RJ, Apkarian AV. Abnormalities in hippocampal functioning with persistent pain. *The Journal of neuroscience : the official journal of the Society for Neuroscience*. 2012; 32(17):5747–5756. [PubMed: 22539837]
100. Naliboff BD, Berman S, Suyenobu B, Labus JS, Chang L, Stains J, Mandelkern MA, Mayer EA. Longitudinal change in perceptual and brain activation response to visceral stimuli in irritable bowel syndrome patients. *Gastroenterology*. 2006; 131(2):352–365. [PubMed: 16890589]
101. O'Mahony SM, Hyland NP, Dinan TG, Cryan JF. Maternal separation as a model of braingut axis dysfunction. *Psychopharmacology*. 2011; 214(1):71–88. [PubMed: 20886335]
102. Pezawas L, Meyer-Lindenberg A, Drabant EM, Verchinski BA, Munoz KE, Kolachana BS, Egan MF, Mattay VS, Hariri AR, Weinberger DR. 5-HTTLPR polymorphism impacts human cingulate-amygdala interactions: a genetic susceptibility mechanism for depression. *Nature neuroscience*. 2005; 8(6):828–834.
103. Pike N. Using false discovery rates for multiple comparisons in ecology and evolution. *Methods Ecol Evol*. 2011; 2(3):278–282.
104. Price DD, Craggs JG, Zhou QQ, Verne GN, Perlstein WM, Robinson ME. Widespread hyperalgesia in irritable bowel syndrome is dynamically maintained by tonic visceral impulse input and placebo/nocebo factors: Evidence from human psychophysics, animal models, and neuroimaging. *NeuroImage*. 2009; 47(3):995–1001. [PubMed: 19375508]
105. Robinson ME, Riley JL 3rd, Myers CD, Sadler IJ, Kvaal SA, Geisser ME, Keefe FJ. The Coping Strategies Questionnaire: a large sample, item level factor analysis. *Clin J Pain*. 1997; 13(1):43–49. [PubMed: 9084951]
106. Rocca MA, Ceccarelli A, Falini A, Colombo B, Tortorella P, Bernasconi L, Comi G, Scotti G, Filippi M. Brain gray matter changes in migraine patients with T2-visible lesions: a 3-T MRI study. *Stroke; a journal of cerebral circulation*. 2006; 37(7):1765–1770.
107. Rodriguez-Raecke R, Niemeier A, Ihle K, Ruether W, May A. Brain Gray Matter Decrease in Chronic Pain Is the Consequence and Not the Cause of Pain. *Journal of Neuroscience*. 2009; 29(44):13746–13750. [PubMed: 19889986]
108. Rubinov M, Sporns O. Complex network measures of brain connectivity: uses and interpretations. *NeuroImage*. 2010; 52(3):1059–1069. [PubMed: 19819337]
109. Sagi Y, Tavor I, Hofstetter S, Tzur-Moryosef S, Blumenfeld-Katzir T, Assaf Y. Learning in the Fast Lane: New Insights into Neuroplasticity. *Neuron*. 2012; 73(6):1195–1203. [PubMed: 22445346]
110. Sanabria-Diaz G, Melie-Garcia L, Iturria-Medina Y, Aleman-Gomez Y, Hernandez-Gonzalez G, Valdes-Urrutia L, Galan L, Valdes-Sosa P. Surface area and cortical thickness descriptors reveal different attributes of the structural human brain networks. *NeuroImage*. 2010; 50(4):1497–1510. [PubMed: 20083210]
111. Schmidt-Wilcke T, Ganssbauer S, Neuner T, Bogdahn U, May A. Subtle grey matter changes between migraine patients and healthy controls. *Cephalalgia : an international journal of headache*. 2008; 28(1):1–4. [PubMed: 17986275]
112. Schmidt-Wilcke T, Leinisch E, Ganssbauer S, Draganski B, Bogdahn U, Altmepfen J, May A. Affective components and intensity of pain correlate with structural differences in gray matter in chronic back pain patients. *Pain*. 2006; 125(1–2):89–97. [PubMed: 16750298]
113. Schmidt-Wilcke T, Leinisch E, Straube A, Kampfe N, Draganski B, Diener HC, Bogdahn U, May A. Gray matter decrease in patients with chronic tension type headache. *Neurology*. 2005; 65(9):1483–1486. [PubMed: 16275843]

114. Schmitt JE, Lenroot RK, Wallace GL, Ordaz S, Taylor KN, Kabani N, Greenstein D, Lerch JP, Kendler KS, Neale MC, Giedd JN. Identification of genetically mediated cortical networks: a multivariate study of pediatric twins and siblings. *Cereb Cortex*. 2008; 18(8):1737–1747. [PubMed: 18234689]
115. Schweinhardt P, Kuchinad A, Pukall CF, Bushnell MC. Increased gray matter density in young women with chronic vulvar pain. *Pain*. 2008; 140(3):411–419. [PubMed: 18930351]
116. Seminowicz DA, Labus JS, Bueller JA, Tillisch K, Naliboff BD, Bushnell MC, Mayer EA. Regional Gray Matter Density Changes in Brains of Patients With Irritable Bowel Syndrome. *Gastroenterology*. 2010; 139(1):48–U82. [PubMed: 20347816]
117. Shattuck DW, Mirza M, Adisetiyo V, Hojatkashani C, Salamon G, Narr KL, Poldrack RA, Bilder RM, Toga AW. Construction of a 3D probabilistic atlas of human cortical structures. *Neuroimage*. 2008; 39(3):1064–1080. [PubMed: 18037310]
118. Shattuck DW, Mirza M, Adisetiyo V, Hojatkashani C, Salamon G, Narr KL, Poldrack RA, Bilder RM, Toga AW. Construction of a 3D probabilistic atlas of human cortical structures. *NeuroImage*. 2008; 39(3):1064–1080. [PubMed: 18037310]
119. Simren M, Barbara G, Flint HJ, Spiegel BM, Spiller RC, Vanner S, Verdu EF, Whorwell PJ, Zoetendal EG. Intestinal microbiota in functional bowel disorders: a Rome foundation report. *Gut*. 2013; 62(1):159–176. [PubMed: 22730468]
120. Smith SM, Jenkinson M, Woolrich MW, Beckmann CF, Behrens TEJ, Johansen-Berg H, Bannister PR, De Luca M, Drobnjak I, Flitney DE, Niazky RK, Saunders J, Vickers J, Zhang YY, De Stefano N, Brady JM, Matthews PM. Advances in functional and structural MR image analysis and implementation as FSL. *NeuroImage*. 2004; 23:S208–S219. [PubMed: 15501092]
121. Soriano-Mas C, Harrison BJ, Pujol J, Lopez-Sola M, Hernandez-Ribas R, Alonso P, Contreras-Rodriguez O, Gimenez M, Blanco-Hinojo L, Ortiz H, Deus J, Menchon JM, Cardoner N. Structural covariance of the neostriatum with regional gray matter volumes. *Brain Struct Funct*. 2013; 218(3):697–709. [PubMed: 22576749]
122. Spielberger, CD.; Gorsuch, RL.; Lushene, R.; Vagg, PR.; Jacobs, GA. *Manual for the State-Trait Anxiety Inventory*. Palo Alto: Consulting Psychologists Press; 1983.
123. Sporns O. Small-world connectivity, motif composition, and complexity of fractal neuronal connections. *Bio Systems*. 2006; 85(1):55–64.
124. Sporns O, Honey CJ. Small worlds inside big brains. *Proceedings of the National Academy of Sciences of the United States of America*. 2006; 103(51):19219–19220. [PubMed: 17159140]
125. Stabell NS, A, Flaegstad T, Nielsen CS. Increased pain sensitivity among adults reporting irritable bowel syndrome symptoms in a large population-based study. *Pain*. 2012
126. Staud R. Abnormal endogenous pain modulation is a shared characteristic of many chronic pain conditions. *Expert review of neurotherapeutics*. 2012; 12(5):577–585. [PubMed: 22550986]
127. Stein JL, Wiedholz LM, Bassett DS, Weinberger DR, Zink CF, Mattay VS, Meyer-Lindenberg A. A validated network of effective amygdala connectivity. *NeuroImage*. 2007; 36(3):736–745. [PubMed: 17475514]
128. Tertulino FF, Goldman SM, Ardengh JC, Lima ER, Ajzen SA, Szejnfeld J, Espirito-Santo DC, Schraibman V, Apodaca-Torrez FR, Lobo EJ. Differentiation of Acute and Chronic Pancreatitis by Diffusion-Weighted Magnetic Resonance Imaging (DW-MRI): A Prospective Study. *Gastroenterology*. 2012; 142(5):S242–S242.
129. Teutsch S, Herken W, Bingel U, Schoell E, May A. Changes in brain gray matter due to repetitive painful stimulation. *NeuroImage*. 2008; 42(2):845–849. [PubMed: 18582579]
130. Thompson PM, Cannon TD, Narr KL, van Erp T, Poutanen VP, Huttunen M, Lonnqvist J, Standertskjold-Nordenstam CG, Kaprio J, Khaledy M, Dail R, Zoumalan CI, Toga AW. Genetic influences on brain structure. *Nature neuroscience*. 2001; 4(12):1253–1258.
131. Thompson, WG.; Longstreth, GL.; Drossman, DA.; Heaton, KW.; Irvine, EJ.; Müller-Lissner, SA. *Functional Bowel Disorders*. In: Drossman, DA.; Corazziari, E.; Talley, NJ.; Thompson, WG.; Whitehead, WE., editors. *Rome II: The Functional Gastrointestinal Disorders Diagnosis, Pathophysiology and Treatment A Multinational Consensus*. Lawrence, KS: Allen Press; 2000.
132. Tillisch K, Labus J, Nam B, Bueller J, Smith S, Suyenobu B, Siffert J, McKelvy J, Naliboff B, Mayer E. Neurokinin-1-receptor antagonism decreases anxiety and emotional arousal circuit

- response to noxious visceral distension in women with irritable bowel syndrome: a pilot study. *Alimentary pharmacology & therapeutics*. 2012; 35(3):360–367. [PubMed: 22221140]
133. Tillisch K, Mayer EA, Labus JS. Quantitative meta-analysis identifies brain regions activated during rectal distension in irritable bowel syndrome. *Gastroenterology*. 2011; 140(1):91–100. [PubMed: 20696168]
134. Tohka J, Dinov ID, Shattuck DW, Toga AW. Brain MRI tissue classification based on local Markov random fields. *Magnetic resonance imaging*. 2010; 28(4):557–573. [PubMed: 20110151]
135. Tohka J, Krestyannikov E, Dinov ID, Graham AM, Shattuck DW, Ruotsalainen U, Toga AW. Genetic algorithms for finite mixture model based voxel classification in neuroimaging. *IEEE transactions on medical imaging*. 2007; 26(5):696–711. [PubMed: 17518064]
136. Torri F, Dinov ID, Zamanyan A, Hobel S, Genco A, Petrosyan P, Clark AP, Liu Z, Eggert P, Pierce J, Knowles JA, Ames J, Kesselman C, Toga AW, Potkin SG, Vawter MP, Macciardi F. Next Generation Sequence Analysis and Computational Genomics Using Graphical Pipeline Workflows. *Genes*. 2012; 3(3):545–575. [PubMed: 23139896]
137. Tracey I, Mantyh PW. The cerebral signature for pain perception and its modulation. *Neuron*. 2007; 55(3):377–391. [PubMed: 17678852]
138. Tu CH, Niddam DM, Chao HT, Chen LF, Chen YS, Wu YT, Yeh TC, Lirng JF, Hsieh JC. Brain morphological changes associated with cyclic menstrual pain. *Pain*. 2010; 150(3):462–468. [PubMed: 20705214]
139. Ung H, Brown JE, Johnson KA, Younger J, Hush J, Mackey S. Multivariate Classification of Structural MRI Data Detects Chronic Low Back Pain. *Cereb Cortex*. 2012
140. Valentino RJ, Miselis RR, Pavcovich LA. Pontine regulation of pelvic viscera: pharmacological target for pelvic visceral dysfunctions. *Trends in pharmacological sciences*. 1999; 20(6):253–260. [PubMed: 10366869]
141. Valfre W, Rainero I, Bergui M, Pinessi L. Voxel-based morphometry reveals gray matter abnormalities in migraine. *Headache*. 2008; 48(1):109–117. [PubMed: 18184293]
142. van Wijk BC, Stam CJ, Daffertshofer A. Comparing brain networks of different size and connectivity density using graph theory. *PloS one*. 2010; 5(10):e13701. [PubMed: 21060892]
143. Wood PB, Glabus MF, Simpson R, Patterson JC 2nd. Changes in gray matter density in fibromyalgia: correlation with dopamine metabolism. *The journal of pain : official journal of the American Pain Society*. 2009; 10(6):609–618. [PubMed: 19398377]
144. Younger JW, Shen YF, Goddard G, Mackey SC. Chronic myofascial temporomandibular pain is associated with neural abnormalities in the trigeminal and limbic systems. *Pain*. 2010; 149(2):222–228. [PubMed: 20236763]
145. Zigmond AS, Snaith RP. The hospital anxiety and depression scale. *Acta Psychiatr Scand*. 1983; 67(6):361–370. [PubMed: 6880820]

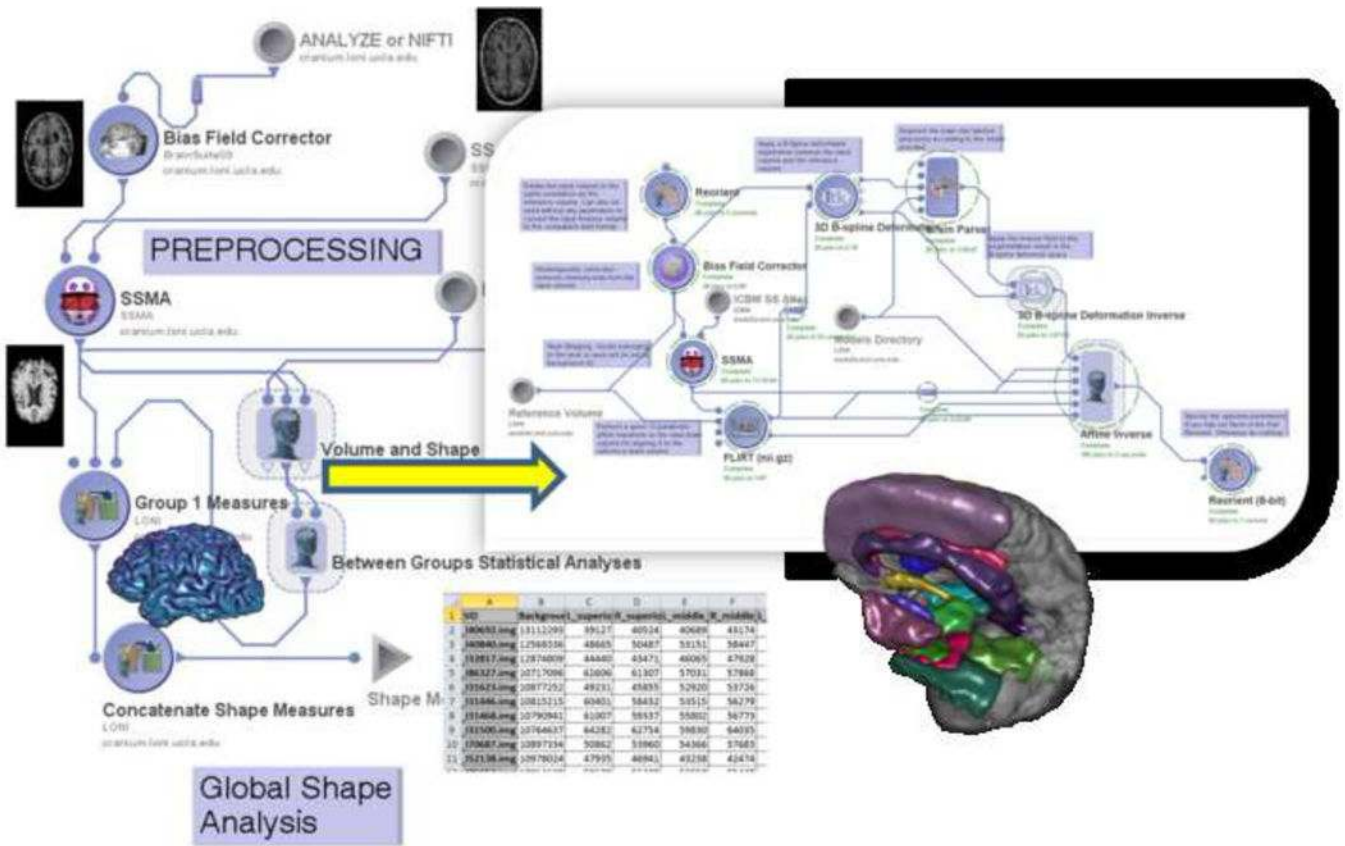


Figure 1.

Volumetric pipeline workflow.

This workflow represents a heterogeneous computational protocol that includes data preprocessing (inhomogeneity correction, skull stripping), brain parcellation, volumetric calculation and statistical analysis of derived neuroimaging biomarkers (i.e., volume) and various subject phenotypes (e.g., diagnosis, age). The insert image illustrates part of the nested processing modules part of the volume and shape processing step of the protocol. Examples of outputs of key processing modules are shown as thumbnail images throughout the workflow. The nodes in the pipeline workflow graph represent atomic processing tools or nested groups of data analysis modules. The edges connecting different nodes in the pipeline graph indicate the data flow and the dependencies of the execution protocol. The volumetric workflow pipeline consists of 4 main components (each annotated by a label) – data preprocessing (intensity inhomogeneity correction and skull-stripping, cortical surface modeling, and tissue classification).

Abbreviations : SSMA- skull-stripping meta-algorithm.

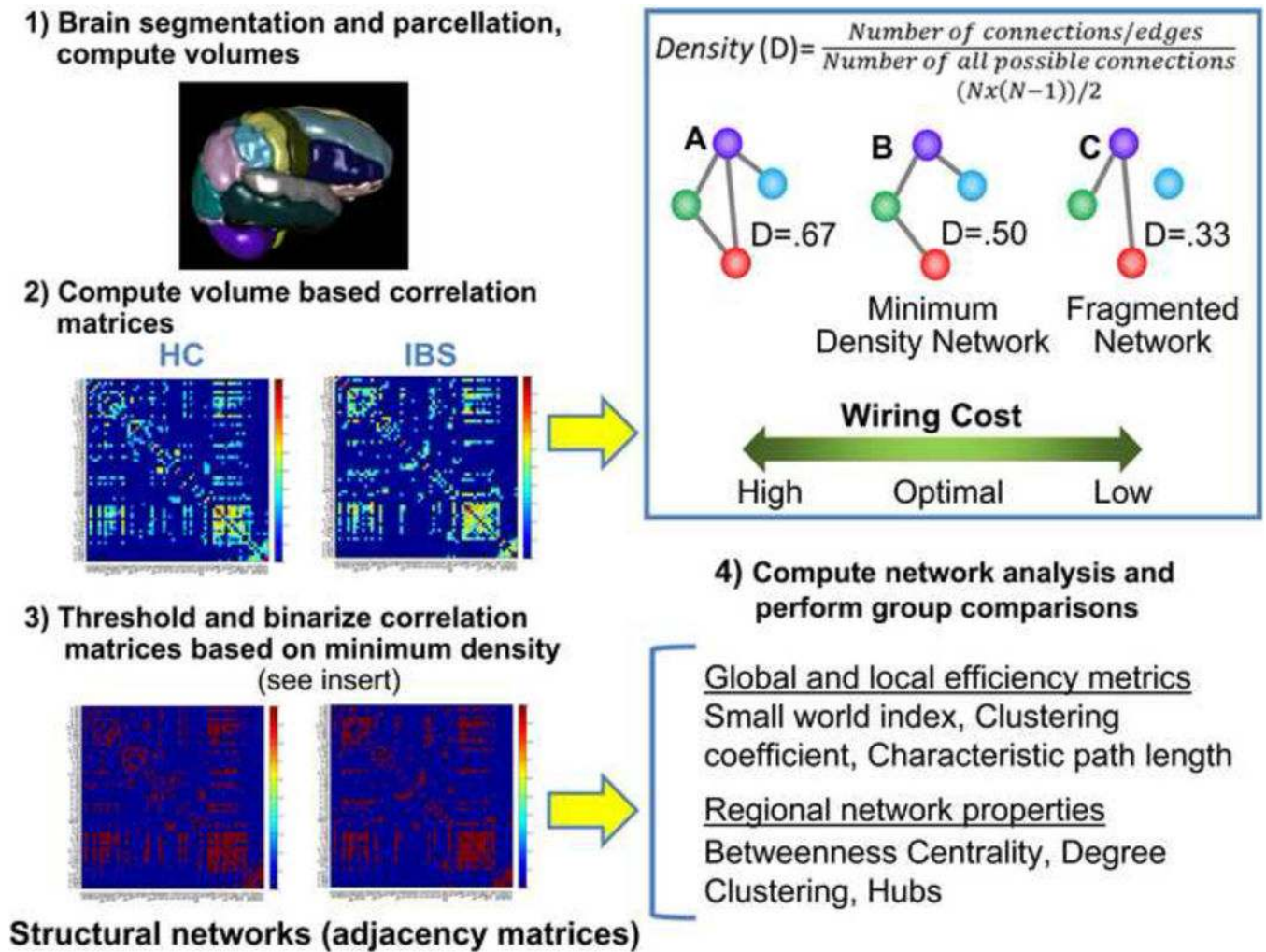


Figure 2.
Network analysis pipeline.

The pipeline consisted of 1) Compute volumes for 62 regions for each subject based on subject-specific brain parcellations using the LPBA 40 and Harvard-Oxford atlases. 2) After controlling for total brain volume with linear regression, inter-regional volume based correlation matrices were computed for each group. 3) Structural brain networks also known as adjacency matrices were then constructed by binarizing the correlation matrices based on the minimum network density threshold (see insert). 4) Based on group adjacency matrices global and regional network metrics and statistical analysis of group differences was performed. Inset. Density is the ratio of the number of connections present to the number of possible connections and is a measure of wiring cost.

Here we present three networks (A,B,C) with varying densities in the context of wiring cost. A minimum density network is a network where all the regions or nodes of the network are fully connected that is, each region has at least one connection). Wiring in the brain is thought to be based on the principle of wiring minimization and cost efficiency which permits the most economical use of space and metabolic costs in the brain. Greater wiring costs (more connections) are associated with greater density (A). Minimum density (B)

reflects the minimum wiring cost possible before network fragmentation (C). The minimum density network is considered to have optimal wiring cost. Abbrev N= connection also called an edge between two regions.

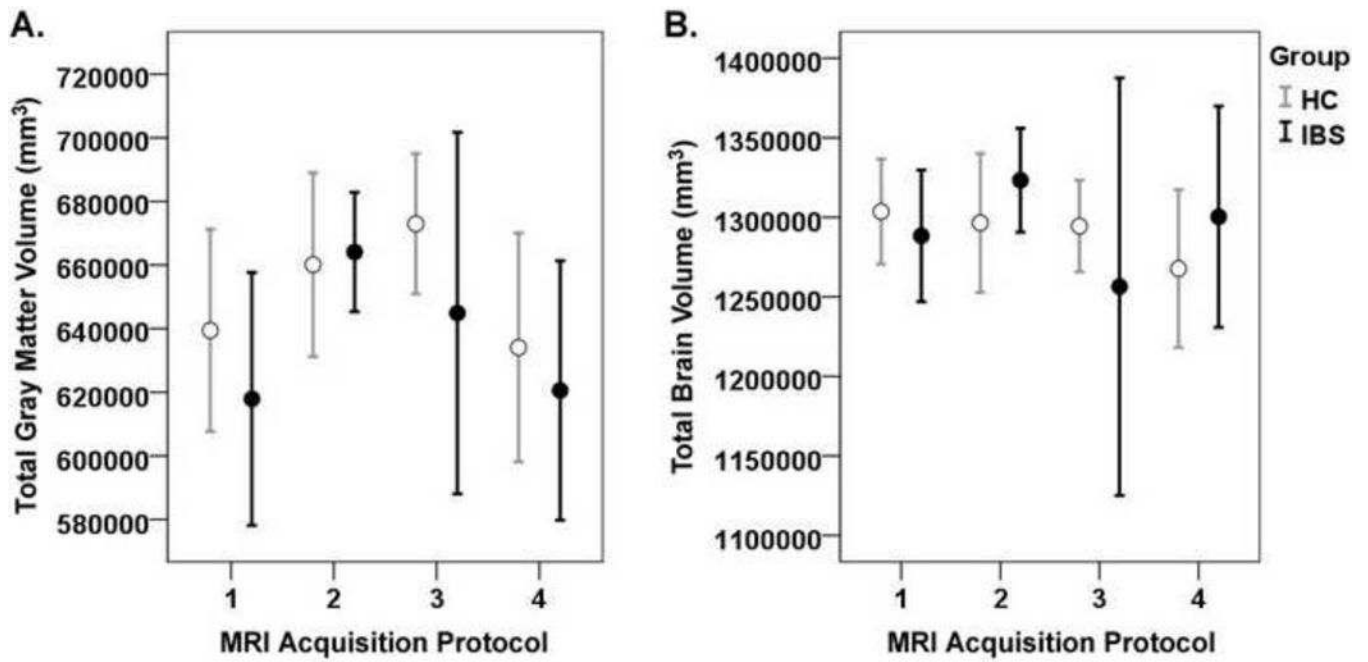


Figure 3.

Gray matter volume by study protocol.

These graphs depicts the mean total grey matter (A) and mean total brain volume (B) and ±95% confidence intervals by acquisition protocol (protocols 1, 2, 3, 4) and group (healthy controls (HCs) and irritable bowel syndrome patients (IBS)). Details of the protocols are described in Table 4.

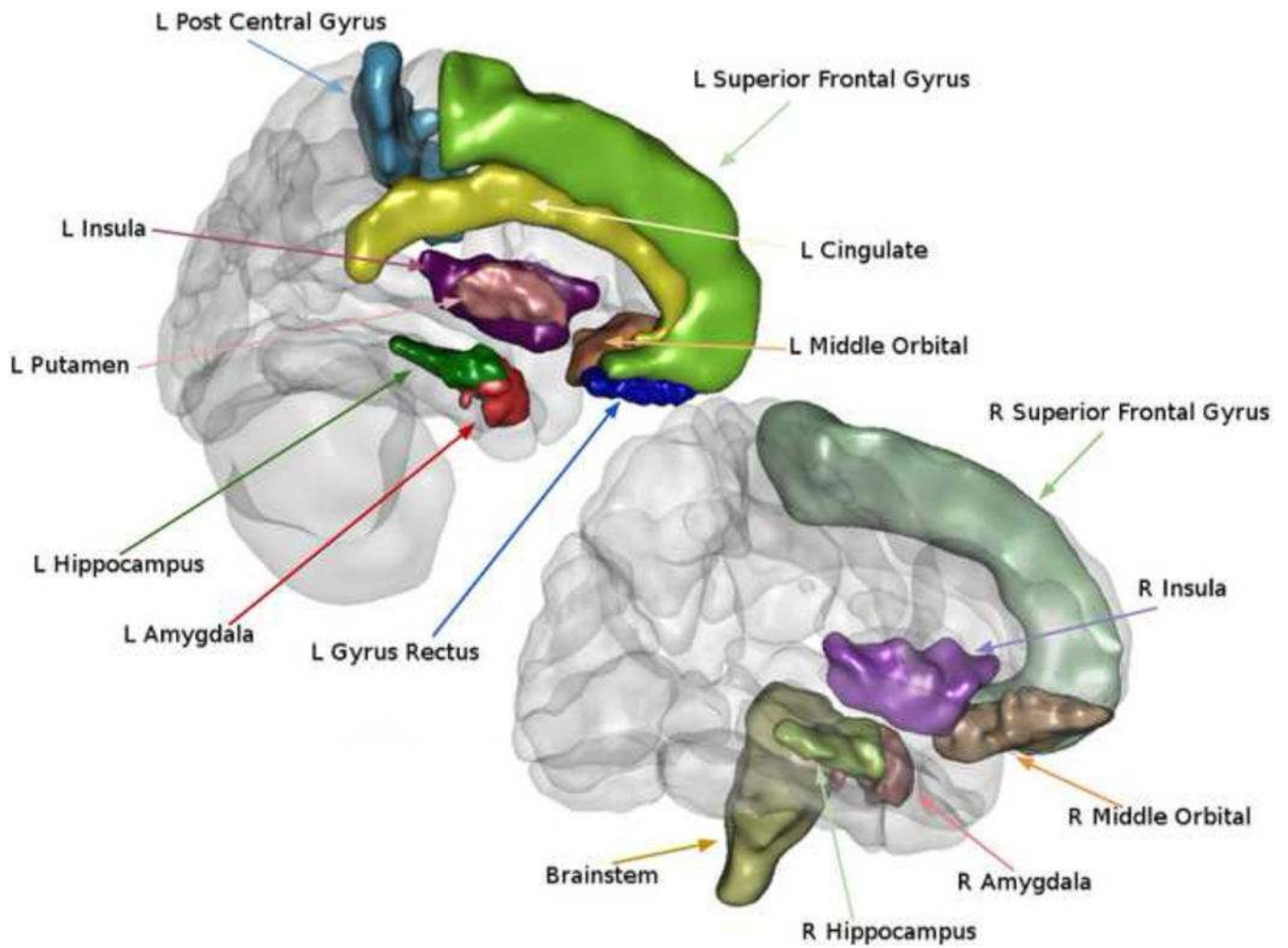


Figure 4. Regions showing volumetric differences between healthy controls and irritable bowel syndrome patients. The atlas-based ROIs that showed group differences are illustrated. ROIs were determined using the LONI probabilistic brain atlas (LBPA 40) and the Harvard-Oxford Atlas.

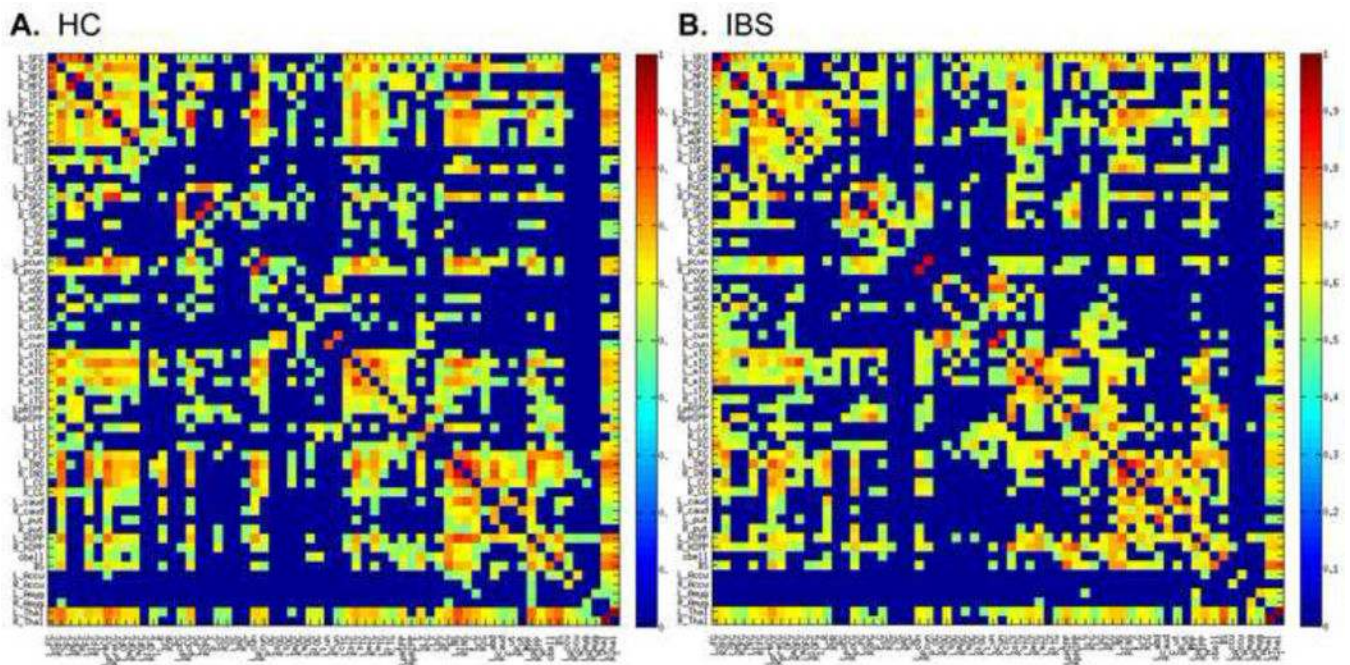


Figure 5.

Thresholded inter-regional correlation matrices. Each colored box represents a correlation between specified brain regions. Abbreviations for brain regions are defined in Table 3. Group specific inter-regional correlation matrices for 62 regional gray matter volumes were thresholded at the minimum density (17%) by setting correlation values to zero where $r < .32$ for irritable bowel syndrome (IBS) and $r < .25$ for healthy controls (HC). In addition, all values across the diagonal of the matrices, representing the correlation of a region with itself were set to zero. Correlation values range from 0 (dark blue) to 1 (dark red).

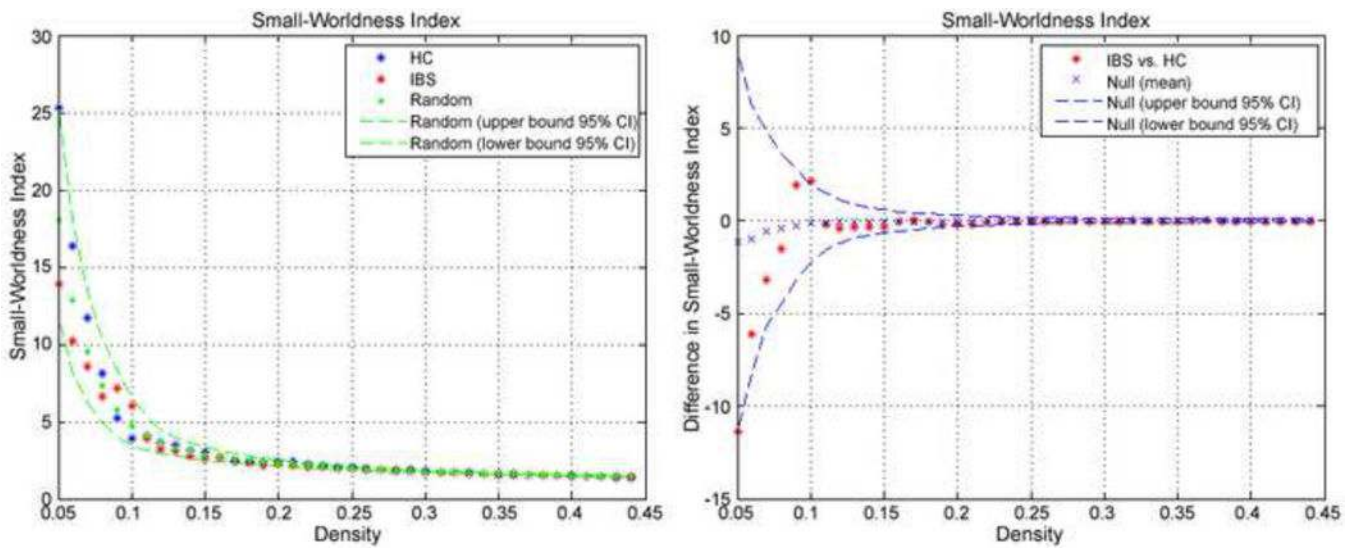


Figure 6. Global network properties of volumetric networks. A) Small world indices across a range of densities. B) Between-group differences and 95% confidence intervals in small-world index as a function of density. Positive values indicate $IBS > HC$ and negative values indicate $IBS < HC$.

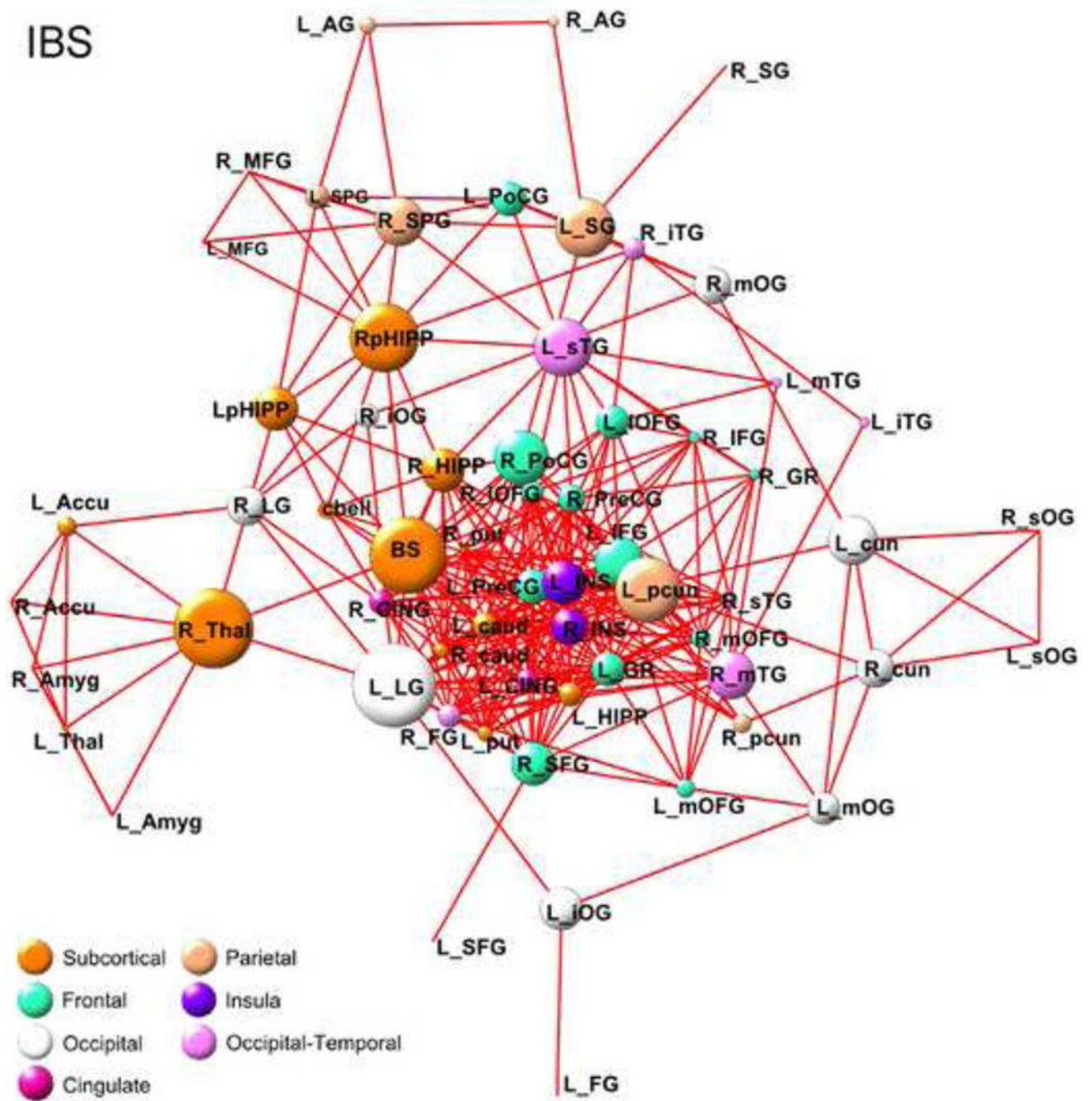


Figure 7. HC and IBS betweenness-based structural network energized using a Kamada-Kawai algorithm. Betweenness is a proportional measure of how often a node (brain region) is located on the shortest path between two brain regions, where shortest path refers smallest distance between two vertices and corresponds to the length (number of edges) between them. Here,

the greater betweenness of a region is depicted by larger circle magnitudes. Edges of the graph represent connected regions. Abbreviations for brain regions are defined in Table 3

Table 1

Structural MRI acquisition protocols

Brain images were obtained from 201 females from 7 structural imaging studies conducted at UCLA using 4 protocols. Abbreviations: HC-healthy control, IBS-irritable bowel syndrome, TR- repetition time, TE- echo time, MRI-magnetic resonance imaging.

	HC (n)	IBS (n)	Age years m(SD) range	Field Strength	TR (ms)	TE (ms)	Flip Angle (°)	Number of Scans
Protocol 1	24	20	29 (11.2) 18 – 64	3 Tesla	20	3.39	25	44
Protocol 2	26	45	31(9.3) 19 – 56	3 Tesla	2300	2.85	9	71
Protocol 3	50	8	32 (9.7) 20 – 56	1.5 Tesla	1900	4.38	15	58
Protocol 4	19	9	30(10.9) 19 – 61	1.5, 3 Tesla	2200	3.26	9	28

Table 2

Distribution of acquisition protocols and subjects across studies.

study	protocol	Subjects
1	1	26
2	1,2,3	14
3	1,2,3,4	108
4	1,2,3,4	25
5	2,4	16
6	4	7
7	2,3	5

Table 3
Cortical and subcortical regions and corresponding abbreviations based on LONI probabilistic brain atlas (LBPA 40) and the Harvard-Oxford atlas

Abbreviations L-left, R-right.

Frontal Lobe		Occipital Lobe	
L superior frontal gyrus	L_SFG	L superior occipital gyrus	L_sOG
R superior frontal gyrus	R_SFG	R superior occipital gyrus	R_sOG
L middle frontal gyrus	L_MFG	L middle occipital gyrus	L_mOG
R middle frontal gyrus	R_MFG	R middle occipital gyrus	R_mOG
L inferior frontal gyrus	L_IFG	L inferior occipital gyrus	L_iOG
R inferior frontal gyrus	R_IFG	R inferior occipital gyrus	R_iOG
L precentral gyrus	L_PreCG	L cuneus	L_cun
R precentral gyrus	R_PreCG	R cuneus	R_cun
L middle orbitofrontal gyrus	L_mOFG		
R middle orbitofrontal gyrus	R_mOFG	Temporal Lobe	
L lateral orbitofrontal gyrus	L_lOFG	L superior temporal gyrus	L_sTG
R lateral orbitofrontal gyrus	R_lOFG	R superior temporal gyrus	R_sTG
L gyrus rectus	L_GR	L middle temporal gyrus	L_mTG
R gyrus rectus	R_GR	R middle temporal gyrus	R_mTG
		L inferior temporal gyrus	L_iTG
Parietal Lobe		R inferior temporal gyrus	R_iTG
L postcentral gyrus	L_PoCG	L parahippocampal gyrus	L_pHIPP
R postcentral gyrus	R_PoCG	R para hippocampal gyrus	R_pHIPP
L superior parietal gyrus	L_SPG	L lingual gyrus	L_LG
R superior parietal gyrus	R_SPG	R lingual gyrus	R_LG
L supramarginal gyrus	L_SG	L fusiform gyrus	L_FG
R supramarginal gyrus	R_SG	R fusiform gyrus	R_FG
L angular gyrus	L_AG		
R angular gyrus	R_AG	Limbic Lobe	
L precuneus	L_pcn	L cingulate gyrus	L_Cing
R precuneus	R_pcn	R cingulate gyrus	R_Cing
		L hippocampus	L_HIPP
Other Structures		R hippocampus	R_HIPP
L insular cortex	L_INS		
R insular cortex	R_INS	Subcortical (Harvard-Oxford Atlas)	
L caudate	L_caud	L Thalamus	L_THAL
R caudate	R_caud	R Thalamus	R_THAL
L putamen	L_put	L Amygdala	L_Amyg
R putamen	R_put	R Amygdala	R_Amyg
Cerebellum	cbell	L Nucleus Accumbens	L_Accu

Frontal Lobe		Occipital Lobe	
Brainstem	BS	R Nucleus Accumbens	R_Accu

Table 4

Demographic and behavioral variables

Mean and standard deviation (SD) for healthy controls (HC) and irritable bowel syndrome (IBS) patients. Patient health questionnaire was score without gastrointestinal items.

	Group	Sample Size	Mean (SD)	Independent sample t-test (df)	p value
Age	HC	119	29.9 (10.3)	-1.59 (199)	.12
	IBS	82	32.2 (9.6)		
Early Trauma Inventory- Global	HC	107	3.3 (3.7)	-1.72 (183)	.09
	IBS	78	4.2 (3.7)		
Anxiety	HC	116	3.8 (3.1)	-3.33 (192)	.001
	IBS	78	5.4 (3.3)		
Depression	HC	116	1.6 (2.3)	-2.67 (192)	.008
	IBS	78	2.6 (2.5)		
Patient Health Questionnaire	HC	76	2.4 (2.0)	-6.99 (121)	1.6 × 10 ⁻⁶
	IBS	47	5.8 (3.3)		
Trait Anxiety	HC	119	45.5 (9.8)	-4.05 (197)	.00007
	IBS	80	51.1 (9.6)		
Catastrophizing	HC	92	0.4 (0.6)	-6.63 (166)	4.4 × 10 ⁻¹⁰
	IBS	76	1.2 (1.0)		

Table 5
Clinical and symptom measures in irritable bowel syndrome (IBS)

Mean and standard deviation (SD) for 82 IBS patients. Information on bowel habit was missing for one subject.

	Sample Size	Mean (SD)
Overall symptom severity past week	75	10.9(4.4)
Abdominal pain past week	77	9.5(4.9)
Usual symptom severity	81	3.2(0.59)
Duration	76	12.7(8.9)

	Frequency Number
Constipation	31(38%)
Diarrhea	22 (27%)
Alternate	16 (20%)
Unspecified	6 (7.0%)
Mixed	5 (6%)

Table 6
Brain regions demonstrating volumetric group differences comparing HC-IBS controlling for total brain volume

F statistics and q value along with standardized effect size, Cohen's d, are reported first from the linear contrast analysis (HC-IBS) on the mean volumetric estimates from the general linear model controlling for total brain volume. Due to the direction of the contrast positive effect sizes represent greater volumes in HCs compared to IBS and negative effect sizes represent greater volume in IBS patients. The last two columns of the table indicate results from linear contrasts analyses after adding the square root of trait anxiety and the square root of global early life trauma scores as covariates to the general linear model controlling for TBV. We report whether group differences in regional volume persisted as indicated by q<.05. Y=denotes regional significance (q<.05) after covariate analysis, N denotes lack of significance. It should be noted that neither trait anxiety of early life trauma scores were considered statistically significant covariates (q<.05) but accounted for enough variance to have effect in the models.

Abbreviations: healthy control- HC, IBS –irritable bowel syndrome, FDR-false discovery rate, SE-standard error

Region of Interest	F (1,198)	FDR Adjusted p q	Mean (mm ³)	SE	Mean (mm ³)	SE	Cohen's d	Group differences remain after controlling for trait anxiety	Group differences remain after controlling for early life trauma
L superior frontal gyrus	4.3	0.029	51401.4	307.0	50407.2	370.0	0.30	Y	N
R superior frontal gyrus	8.5	0.006	54705.5	440.1	52689.6	530.3	0.42	Y	N
L cingulate	9.5	0.006	11358.7	142.1	10673.0	171.3	0.44	Y	N
Braunstem	4.9	0.024	26649.4	255.1	25766.7	307.5	0.32	N	N
L insula	7.6	0.008	8310.9	101.3	7874.0	122.1	0.40	Y	N
R insula	10.3	0.006	5510.5	87.1	5071.9	105.0	0.46	Y	N
L middle orbital frontal gyrus	6.5	0.012	8618.3	71.0	8335.4	85.6	0.37	Y	N
R middle orbital frontal gyrus	5.2	0.021	9361.6	84.0	9060.3	101.2	0.33	Y	N
L gyrus rectus	7.9	0.007	2078.9	40.8	1898.9	49.2	0.61	Y	N
L hippocampus	8.6	0.006	3674.8	37.5	3502.0	45.2	0.42	Y	N
R hippocampus	8.5	0.006	4008.6	30.7	3868.9	36.9	0.42	Y	N
L Putamen	6.8	0.011	2909.1	59.5	2666.5	71.7	0.38	Y	N
L amygdala	4.4	0.028	1224.9	24.0	1145.4	28.9	0.31	Y	N
R amygdala	9.3	0.006	1219.8	25.7	1096.7	31.0	0.44	Y	Y
L post central gyrus	14.1	0.003	20134.9	220.3	21431.5	265.5	-0.54	Y	Y

Table 7
Network metrics at minimum density

Global network measures for healthy control (HC) and irritable bowel syndrome (IBS) structural networks at the minimum density =.17.

	HC	IBS	pval
Mean Degree	11.0	11.0	0.99
Mean Clustering Coefficient	0.57	0.52	0.38
Normalized Clustering Coefficient	3.23	3.00	0.38
Global Efficiency	0.49	0.50	0.99
Mean Local Efficiency	0.70	0.64	0.43
Modularity	0.28	0.28	0.36
Characteristic Path Length	2.55	2.42	0.20
Normalized Path Length	1.34	1.27	0.20
Mean Node Betweenness	97.2	88.8	0.26
Mean Edge Betweenness	2.55	2.42	0.30
Small Worldliness	2.41	2.36	0.20